Decellularized Extracellular Matrix (dECM) Microparticle Based Hydrogels for Vocal Fold Tissue Engineering

Mika Brown

Biological and Biomedical Engineering

McGill University, Montréal

Submitted December 2018

A thesis submitted to McGill University in partial fulfillment of the requirements of the degree of Master of Engineering (M. Eng)

Table of Contents

i. List of Figures

ii. List of Tables

iii. Abstract

Vocal fold (VF) atrophy and scarring cause permanent tissue loss or recalcitrant fibrotic changes in the tissue. Affected individuals may lose their voices completely. Therapeutic applications of bioengineered hydrogels have been proposed to restore the damaged extracellular matrix (ECM) with similar mechanical and bioactive properties to the native tissue. Major ECM components such as collagen, elastin and hyaluronic acid (HA) need to be recovered because of their important roles in structural support and cell signaling processes. Previous attempts were made to decellularize the ECM of small intestine submucosa (SIS) and reconstitute it to an injectable hydrogel. However, the ECM composition of SIS is different from that of the VF. The primary goal of this thesis was to investigate the biological and mechanical properties of an ECM-based hydrogel derived from porcine VF in the treatment of severe VF injury and damage.

Porcine VF were dissected from larynges obtained from a local abattoir. The VF tissue was decellularized, homogenized, and digested to enable gelation. Eight ECM decellularization protocols were tested by varying exposure time to 0.75 mg/mL deoxyribonuclease (DNase), or both DNase and 0.1 mg/mL ribonuclease (RNase). Homogenization was executed in a tissue lyser using ceramic beads to create decellularized ECM (dECM) microparticles. Preservation of collagen, elastin, and HA was assessed using biochemical assays. Microparticles were solubilized with pepsin, neutralized with sodium hydroxide, and incubated to induce gelation at concentrations of 0.5%, 1.0%, and 1.5% dECM. Immortalized human vocal fold fibroblasts (HVFF) were encapsulated in the hydrogels and subjected to cell viability tests up to 7 days. Mechanical properties were determined by linear-shear rheometry and swelling tests. Surface characteristics of the hydrogel were observed under Environmental Scanning Electron Microscopy. Enzymatic degradation kinetics were determined using 0.05% collagenase.

The decellularization protocol wherein VF were exposed to both DNase and RNase for 48 h was maximized, as > 95% of DNA content was consistently removed. Although collagen content was not altered significantly from native VF concentration by decellularization or homogenization, both elastin and HA content were reduced. Rheological characterization showed that only the 1.5% dECM hydrogel met the mechanical requirements for a VF biomaterial, with a storage modulus above 100 Pa and capable of withstanding > 30% strain. However, all three dECM hydrogels contracted over time comparably to a collagen-HA (CHA) control and degraded rapidly. Additionally, HVFF encapsulated in the 1.5% dECM hydrogels did not appear healthy after 1, 3 and 7 days of culture. Results from this thesis work suggested that VF-dECM hydrogels would require further development to improve mechanical tunability and decrease ECM composition alterations and degradation rate for application in VF tissue reconstruction.

iv. Résumé

L'atrophie et les cicatrices de la cordes vocales (CV) causent une perte permanente des tissus ou des modifications fibreuses récalcitrantes dans les tissus. Les personnes affectées peuvent perdre complètement leur voix. Des applications thérapeutiques d'hydrogels issus de la bio-ingénierie ont été proposées pour restaurer la matrice extracellulaire (MEC) endommagée avec des propriétés mécaniques et bioactives similaires au tissu natif. Les composants principaux de la MEC tels que le collagène, l'élastine et l'acide hyaluronique (HA) doivent être collectés en raison de leur rôle important dans les processus de support structurel et de signalisation cellulaire. Des études antérieures ont déjà essayé de décelluleriser la MEC de la sous-muqueuse de l'intestin grêle (SIS) et la reconstituer en un hydrogel injectable. Cependant, la composition de la MEC du SIS est différente de celle du CV. L'objectif principal de cette étude est donc d'étudier les propriétés biologiques et mécaniques d'un hydrogel à base de MEC dérivé de la CV porcine dans le traitement des lésions et des dommages graves causés à la CV.

Pour ce faire, des CV porcins ont été disséqués à partir de larynges obtenus d'un abattoir local. Le tissu CV a été décellularisé, homogénéisé et digéré pour permettre sa gélification. Huit protocoles de décellularisation de MEC ont été testés en faisant varier le temps d'exposition à la désoxyribonucléase (DNase) 0,75 mg / mL, ou simultanément à la DNase et à la ribonucléase (RNase) 0,1 mg / mL. L'homogénéisation a été réalisée dans un broyeur de tissu utilisant des billes de céramique pour créer des microparticules de MEC décellularisées (dMEC). La préservation du collagène, de l'élastine et de l'HA a été évaluée à l'aide d'analyses biochimiques. Les microparticules ont été solubilisées avec de la pepsine, neutralisées avec de l'hydroxyde de sodium et incubées pour induire la gélification à des concentrations de 0,5%, 1,0% et 1,5% de dMEC. Des fibroblastes de cordes vocales humaines immortalisés (HVFF) ont été encapsulés

dans les hydrogels et testés pour déterminer leur viabilité pendant une période allant jusqu'à 7 jours. Les propriétés mécaniques ont été déterminées par des tests de rhéométrie par cisaillement linéaire et de gonflement. Les caractéristiques de surface de l'hydrogel ont été observées par microscopie électronique à balayage. La cinétique de dégradation enzymatique a été déterminée en utilisant 0,05% de collagénase.

Les protocoles de décellularisation où les CV ont été exposées à la fois à la DNase à la RNase pendant 48 h ont été maximisé, étant donné que plus de 95% du contenu en DNA était systématiquement éliminé. Bien que le contenu en collagène n'était pas significativement altéré par la décellularisation ou l'homogénéisation comparativement à sa concentration dans les CV natives, les teneurs d'élastine et d'HA ont été réduites. La caractérisation rhéologique a montré que seul l'hydrogel à 1.5% de dMEC correspondait aux exigences mécaniques d'un biomatériau pour la CV, avec un module de conservation supérieur à 100 Pa et capable de supporter une contrainte supérieure à 30%. Cependant, les trois hydrogels de dMEC se contractaient avec le temps, de manière comparable au collagène-HA (CHA) témoin et se dégradaient rapidement. De plus, de HVFF encapsulés dans les hydrogels à 1,5% de dMEC ne semblait pas sains après 1, 3 et 7 jours de culture. Les résultats de cette thèse suggèrent que les hydrogels PV-dMEC nécessiteraient des travaux supplémentaires, tels que l'amélioration de la modulabilité mécanique, la réduction du nombre d'altérations de la composition de la MEC, ainsi que la diminution du taux de dégradation, pour leur application à la reconstruction de tissu de CV.

v. Acknowledgements

I would like to acknowledge all those who helped me in the process of completing the research, analysis, and documentation I performed during my Master's thesis. First, I would like to thank my primary thesis advisor, Dr. Nicole Li-Jessen, who encouraged me to develop my research plan independently and always gave excellent and supportive feedback on my work. She made time every week to ensure my research was progressing on track and helped direct me to available resources when I needed assistance. My co-supervisor, Luc Mongeau, enabled my participation in the BBME program and provided me the use of his equipment. I would also like to thank the members of the Li-Jessen Lab and Mongeau lab, especially Patrick Coburn for his cell culture training and invaluable advice on cell staining and analysis. Chelsea Ridgeway, an undergraduate summer intern, provided assistance with microparticle production and the completion of biochemical assays. Another undergraduate researcher, James Cui, provided my initial training on the cryostat and in histology protocols. Dr. Huijie Wang, Mongeau's lab manager, organized the purchase of necessary materials and helped me locate equipment, which helped ensure that I was able to complete experiments. Guangyu Bao and Hossein Ravanbakhsh provided rheometer training, assistance with rheology protocol troubleshooting, and advice on results interpretation. I received scanning electron microscopy training from Dr. David Liu from McGill's Facility for Electron Microscopy and further assistance from Dr. Kelly Sears. Dr. Nelly Vuillemin and Dr. Erika Lee provided my training in wide-field and confocal microscopy. Project funding was granted thanks to the Natural Sciences and Engineering Research Council of Canada RGPIN-2018-03843 (Li-Jessen) and the National Institute on Deafness and Other Communication Disorders R01 DC005788 (Mongeau).

vi. Contribution of Authors

The research described herein was planned, carried out, and compiled by Mika Brown. Assistance in data collection and analysis was received as described in the acknowledgements, but Mika was the primary contributor to all work contained herein. Editing was completed with the assistance of Dr. Nicole Li-Jessen, including some suggested wording.

Chapter 1. Introduction

1.1. Rationale

Approximately 3% - 9% of the general population have a voice disorder[1]. Damaged vocal folds (VF) require a treatment that can augment their phonatory function long-term and reduce the formation of fibrotic tissue. The composition and structure of VF is highly specific, and changes in composition disrupt VF oscillation for phonation. Hydrogels consisting of extracellular matrix (ECM) derived proteins and glycosaminoglycans (GAGs) have been explored to replace impaired VF[2,3]. These hydrogels contain only one or two ECM proteins, most frequently collagen I or hyaluronic acid (HA), which do not replicate the complex composition of native VF. A decellularized extracellular matrix (dECM)-hydrogel is proposed herein as a potential injectable biomaterial for VF scarring. dECM hydrogels derived from VF may more accurately reproduce the structure and function of VF because they possess most components of the native ECM.

Decellularized scaffolds have been suggested to promote an anti-inflammatory immune response, preserve organization of structural collagens, and retain growth factors, cytokines, and other bioactive molecules that can stimulate the regeneration of functional tissue complete with nerves and blood vessels[4,5]. More specifically, dECM hydrogels have been shown to promote local M2 phenotype macrophage responses and upregulate cytokines such as interleukin-4 (IL-4) that enhance constructive tissue remodeling. Scaffolds composed of porcine small intestinal submucosa (SIS) and urinary bladder matrix (UBM) dECM are developed for clinical applications in wound healing, such as to treat skin, bone, and gastrointestinal damage. Xenogeneic dECM scaffolds were proposed to circumvent organ shortages from human donors.

No adverse impact on the regenerative responses the millions of patients treated with xenogeneic dECM scaffolds has been observed thus far[6].

The primary components of human VF ECM are collagens I and III, and elastin[2]. VF also contain a particularly high concentration of HA, a GAG that protects the VF against damage from vibration. Although some GAGs are always lost during decellularization, dECM has been suggested to retain the specific composition of the source tissue's ECM[7]. Previous dECM hydrogels for VF tissue engineering have been fabricated from small intestine submucosa (SIS), a mucosal tissue with some composition similarities to the VF lamina propria (LP)[8,9]. At the same time, results from other dECM studies suggested the source of dECM is imperative for the generation of an effective regenerative response when using dECM-derived hydrogels[7,10,11].

As the ECM compositions of SIS and VF lamina propria are not identical, using VF-derived dECM hydrogels may provide a more effective platform to replicate the unique anatomical and biomechanical properties of VF[12]. The importance of these differences has not yet been investigated for VF tissue engineering. Further, porcine VF possessed the greatest compositional similarity to human VF compared to other animals[13,14]. In this thesis, three research aims were proposed to develop dECM hydrogels from porcine VF and characterize the biochemical and mechanical properties of these materials.

1.2. Objectives

Aim 1. To evaluate the effectiveness of decellularization ECM protocols for porcine VF. Eight dECM protocols with varying concentrations of RNase, total nuclease exposure time and total peracetic acid exposure time were performed on porcine VF. The residual DNA content of the dECM was quantified to evaluate the effectiveness of cell removal from the porcine VF.

Aim 2. To evaluate the effectiveness of homogenization protocol for VF-dECM microparticles. Microparticles were produced by milling the whole VF-dECM in a tissue lyser with varying sizes of ceramic beads. The yield of dECM microparticles and their collagen, elastin, and HA concentrations were quantified to evaluate the effectiveness of the homogenization protocol.

Aim 3. To evaluate the biocompability and mechanical properties of VF-dECM hydrogels. VF-dECM hydrogels were fabricated at concentrations of 0.5%, 1.0%, and 1.5% dECM microparticles using pepsin solubilization. Mechanical properties including gelation time, swelling, and degradation kinetics were evaluated. Cell viability of human VF fibroblasts (HVFF) was evaluated after 1, 3, and 7 days of culture inside the VF-dECM hydrogel.

Chapter 2. Comprehensive Literature Review

2.1. Vocal Fold Anatomy, Disorders and Conventional Treatments

Human vocal folds (VF) are pairs of 3-10 mm thick soft, connective tissues located within the larynx that are responsible for both phonation and airway protection[15,16]. Each VF consists of three layers: the innermost thyroarytenoid muscle, intermediate stratified squamous epithelium, and the mucosal lamina propria (LP)[17]. The LP itself has three layers: deep, intermediate, and superficial, of which the superficial layer is most involved in sound production. During phonation, the superficial LP oscillates over the lower layers in a small amplitude wave to generate sound in concert with the larynx, trachea, and vocal cavities.

The distinct, multicomponent ECM of the LP enables the VF to vibrate over frequencies of 60-1000 Hz for human phonatory and singing functions[15,16]. The flexibility of elastin and the basket-like structure of collagen fibers grants VF the ability to reversibly elongate under up to 30% strain[18,19]. Collagen comprises 40-50% of human VF total protein. Compared to other soft tissues, which are generally rich in collagen I, the concentration of collagen III is particularly high in healthy adult VF-LP[15]. The concentration of elastin, 6-10% of the total protein, is also notably high in VF[13]. Hyaluronic acid (HA), a linear, non-sulfated glycosaminoglycan present in VF ECM in smaller quantities, ~0.8% of total protein, protects VF against trauma by absorbing impact shock and damping VF edges during vibration[13,16,20]. Other ECM substrates include membrane proteins, such as fibrin and laminin, proteoglycans, such as heparin, and small molecules. The most common cell type in VF is VF fibroblasts, which are necessary to sustain ECM homeostasis within the LP[17]. An imbalance in ECM homeostasis is frequently related to the development of VF disorders such as scarring and atrophy.

2.1.1. Impact of Common Disorders

As high as 9% of the United States population has a voice disorder, with 29% expected to develop one during their lifetime[16,17,21]. Environmental and pathological conditions can alter the composition of VF-LP through a variety of mechanisms, resulting in voice disorders that hamper phonation and negatively impact quality of life. These pathologies can result from professional hazards such as voice over use in teachers and singers, and exposure to chemicals or radiation. Injuries and common inflammatory disorders including allergies, asthma, and gastroesophageal reflux may also damage VF. Symptoms frequently include hoarseness, discomfort when speaking, and vocal fatigue, hampering an individual's communication ability and quality of life.

Recalcitrant fibrotic changes to the ECM caused by these pathologies impede the oscillations of the superficial LP[16]. Incomplete VF adduction, or glottal insufficiency, can result from these changes, impairing the ability of VF to both protect the airway and generate sound. Because VF stiffness impacts the ability of the LP to vibrate, fibrotic scarring can impede phonation. Changes in elastin organization may also reduce the ability of VF to vibrate and stretch effectively for phonation[15]. VF possess a limited aptitude for regeneration, meaning many of these pathological changes are permanent[17]. Several treatment methods currently exist for different types of voice disorders. However, an effective, long-term, regenerative treatment method has not yet been discovered.

2.1.2. Conventional Voice Treatments

Current treatments for VF disorders include surgery, drug or biomaterial injection, and behavioral voice therapy[22]. Behavioral voice therapy is used to limit disease progression or further injury through vocal training exercises to reduce vocal fatigue and improve voice quality.

Behavioral modifications are also prescribed to manage any medical and lifestyle factors, such as acid reflux, allergies, and voice use patterns that affect vocal health. These techniques do not treat the source of the pathology but may improve quality of life for patients with voice disorders.

Surgery is typically performed to remove nodules, repair glottal insufficiency, or implant tissue grafts[16,23]. Injection laryngoscopy involves the insertion of a laryngoscope to the larynx, and injection of biomaterials such as calcium hydroxylapatite into the LP. This technique is most effective in restoring some vibratory capacity to VF with mild or moderate scarring. However, the injected biomaterials degrade over time without sufficiently replacing native tissue, and recurring injections may be required. Both surgical and injection procedures may cause additional fibrotic scarring on VF. While these methods may ameliorate symptoms, a treatment that regenerates damaged VF ECM has not yet been developed. A range of biomaterials for VF tissue engineering are under development to overcome the shortcomings of conventional treatments for VF disorders.

2.2. The State of Art in VF Tissue Engineering

The overarching challenge of VF tissue engineering is replicating both the distinct mechanical and bioactive properties of native VF within a single material[20]. In pursuit of this goal, investigators have designed materials that blend bioactive molecules (e.g. membrane proteins or GAGs) and stem cells within injectable materials. However, a biomaterial that successfully replicates both the mechanical and bioactive properties of VF has yet to be developed. Such a material must be ample to sustain repeated, reversible deformation under 30% strain at high frequency for long durations, and function as a barrier to protect the airway[24].

The primary factors to consider when designing a biomaterial for VF tissue engineering are tunability of mechanical properties and availability of bioactive molecules to stimulate cellular adhesion and control material biodegradation[20,25]. Injectable hydrogels are also preferable to minimize invasiveness and the risk of further scarring. Hydrogels are pliable materials with high water content that are capable of filling completely filling gaps in tissue, desirable properties for biomaterials used in soft tissues including VF.

2.2.1. Materials Used in Vocal Fold Tissue Engineering

Selection of appropriate components for scaffolds intended to stimulate VF regeneration is essential[15,20]. It is important that the biomaterials selected possess viscoelastic properties within the range of native human VF (storage modulus (G') = 0.1 -1 kPa) as greater moduli impair LP vibration and sound production. The native viscoelastic moduli vary across this range depending on many factors including frequency of phonation, gender, and age. Severe inflammatory responses can result from poor material choice.

While synthetic polymers such as polyethers or polyurethanes possess highly tunable mechanical properties, they lack bioactive molecules that promote cellular interactions including adhesion, infiltration, and tissue-scaffold integration[16]. For this reason, VF tissue engineering has largely focused on naturally-derived biomaterials, particularly ECM components such as collagen and hyaluronic acid, and composites of these materials with polymers. The risks of using ECM component-derived materials include batch-to-batch composition changes, and a lesser degree of tunability compared to synthetic materials.

Collagen hydrogels can be produced by reconstituting native collagen I from bovine or rat tail. These hydrogels possess stable mechanical properties and are favorable for cell proliferation[26]. Collagen-HA co-gels, produced as a simple 1:1 mixture of their respective pre-gel solutions,

were found to reduce early signs of inflammation and stimulate the production of structurally organized ECM after twelve months when adipose stem cells (ASC) were cultured on their surface. However, excess deposition of disorganized collagen was observed after three months[27]. Further, the relevance of this scaffold to VF regeneration was not comprehensively evaluated. Neither the impact of the gel on ASC differentiation into cells found within the VF nor the recovery of VF vibratory properties were measured. A significant drawback of collagen hydrogels is that they are reabsorbed into tissue over time. In one study, a co-gel of collagen and HA, formed by mixing the two materials and incubation, stimulated cell proliferation over an alginate and collagen co-gel, but much of the collagen-HA was resorbed into tissue over only 28 days *in vitro*[26]. In contrast, the collagen-alginate gel was stable for 42 days and stimulated ECM deposition. These results indicate that collagen in composite with a more slowly degrading, resorption-resistant biomaterial may enhance hydrogel stability, and produce more favorable long-term results for VF regeneration.

Chemically-crosslinked composites have been designed to increase the physiological stability of collagen-based materials[26]. This is favorable because native collagen assemblies are organized by crosslinking with lysyl oxidase. Collagen-HA hydrogels were fabricated through two methods by Farran et al: (1) mature collagen fibrils supported by HA oxidized with sodium periodate, and (2) immature collagen fibrils crosslinked with HA modified with adipic acid dihydrazide using carbodiimides[28]. When HVFF were encapsulated in the gels, both stimulated cell proliferation, elongation into native fibroblast morphology, and ECM deposition. While HA degraded over time in both gels, crosslinking significantly decreased the rate of degradation, which helped maintain the viscoelasticity of the hydrogel over time.

Glutaraldehyde-crosslinked collagen-gelatin sponges, containing basic fibroblast growth factor (bFGF) were synthesized as an implantable scaffold for VF tissue engineering[29]. Although bFGF has been shown to trigger a VF repair, this effect cannot be exploited without a mechanism for sustained release, because bFGF is rapidly absorbed into tissue. Collagen-gelatin sponges have previously been used to control the release of bFGF in skin tissue engineering, a scaffold that stimulated dermis regrowth and capillary formation and proceeded to clinical trials. The collagen-gelatin sponge containing encapsulated bFGF improved HA and elastin deposition, decreased excess collagen production, and increased the amplitude of VF vibration in a canine model over bFGF injection or the collagen-gelatin scaffold alone. Despite these favorable outcomes, it is important to recognize that common crosslinkers such as carbodiimides and glutaraldehyde can produce toxic byproducts as scaffolds break down *in vivo* or crosslink DNA and proteins[30,31].

Despite the important role of elastin in sustaining VF oscillation, native elastin is rarely used in scaffold development because it is challenging to extract and may lose its stability and cell-signaling abilities if broken into fragments[32]. Elastin's hydrophobic nature also complicates the fabrication of hydrogels, where a pre-gel solution is required for scaffold formation. Nevertheless, elastin is a long-lasting protein with a half-life of 70 years and is generally not produced in functional adult tissue. Elastin and elastin-like materials remain of key interest for VF tissue engineering. Synthetic biodegradable elastomers, recombinant tropoelastin, and elastin-based peptides have been used as alternatives to native elastin[32].

Although native HA degrades within 3-5 days of injection into the VF, crosslinked and composite HA-derived materials such as Genzyme's Hylaform® have been clinically investigated[16]. While Hylaform® was available in the United States in the early 2000s and was

able to improve phonation in patients with disordered voice, it has since been taken off the market. One composite crosslinked di (thiopropionyl) bishydrazide-modified HA with di(thiopropionyl) bishydrazide modified gelatin using polyethylene glycol diacrylate (PEGDA) to repair scarring in the LP[1]. This hydrogel interacted with human VF fibroblasts (HVFF) in a similar manner to how HA recruits cells during wound healing and stimulated ECM deposition. In general, HA-based hydrogels improve VF function without eliminating the sources of the problem, such as fibrotic scarring[20].

Injectable biomaterials that more accurately replicates the composition, structure, and bioactive and mechanical properties of VF are expected to induce effective integrative and regenerative responses[25,33]. Composites of multiple proteins have demonstrated to possess more dynamic mechanical properties and fulfil a wider range of functions than single-protein hydrogels. In collagen-elastin composites, the strength of collagen and viscoelastic properties of elastin can be combined to provide the environmental niches required for tissue function. In an *in vitro* study, Sionkowska et al. altered the ratio of collagen and elastin to create skin grafts with either greater tensile strength or elasticity and resilience[34]. Notably, the surface interactions between cells and the scaffold were altered along with the collagen-elastin ratio. Scaffolds composed of collagen fibrils coated with elastin were clinically evaluated for skin regeneration following severe burns[35]. Patients did not develop hematomas and recovered full range of motion at a 12 month follow up, though three of the original patients were unable to participate in the follow-up due to death (respiratory insufficiency, resurgence of carcinoma) or change of address. This skin graft is currently sold by MedSkin Solutions on the commercial market under the name Matriderm®[36].

Despite these successes in skin tissue engineering, the wide variety of protein-protein interactions that occur within ECM, including electrostatic, hydrogen bonding, and hydrophobic-

hydrophilic effects, cannot be replicated with a single or two proteins[25]. This is particularly true for more complex tissues, including VF. One solution suggested for this shortcoming is the use of decellularized ECM, which contains most necessary native proteins, but can be treated as a single material, and can be used alone, modified, or in composite with another material.

2.3. Decellularized Extracellular Matrix in Vocal Fold Tissue Engineering

The primary rationale for the application of decellularized extracellular matrix (dECM) to tissue engineering applications is the retention of ECM structural and functional components[37]. These components include not only the primary structural components of ECM – collagen and elastin – but proteoglycans, GAGs, growth factors, and cytokines, each of which stimulate unique cell-tissue and tissue-tissue interactions. These components are concentrated in specific locations within specific types of ECM[38]. There is no comprehensive understanding of the precise interactions between each component of the ECM and the surrounding environment, which increases the difficulty of replicating the tissue-specific interactions for varying tissue types from synthetic and simple protein composites. However, the use of native ECM in tissue engineering applications requires decellularization, a process that must be tuned to eliminate allogenic or xenogeneic cells, which contain nucleic acids and immunogenic proteins capable of causing severe immune responses[37].

Initial concerns were expressed regarding the use of xenogeneic ECM biomaterials in humans due to the presence of the Gal epitope, to which humans have a strong adverse immune response. So far, only a trace of this epitope has been found in dECM scaffolds[6]. No adverse effects have been attributed to adverse responses to xenogeneic epitopes in any of the dECM scaffolds currently on the market. Moreover, dECM scaffolds have demonstrated the ability to stimulate polarization of macrophages to the M2 phenotype and increase generation of IL-4, markers of

constructive remodeling and a beneficial immune response[4]. However, insufficient decellularization or lack of contact with adjoining tissue following implantation can lead to a pro-inflammatory response and chronic inflammation, emphasizing the importance of scaffold fabrication and design.

The first decellularized tissues developed were urinary bladder matrix (UBM) and small intestine submucosa (SIS), both of which are currently used in a variety of clinically approved wound healing applications[4]. UBM-based products are on the market for treatment of severe burns, a variety of gastrointestinal applications, including repair of the abdominal wall, and to bolster bladder and gynecologic tissues. In a preclinical study, ACell's Matristem UBM™ scaffold was administered to three patients with deep burns covering an average surface area of 7.2% of their bodies, and burned areas seeded with epithelial cells 4-7 days after treatment[39]. Complete recovery from burns was achieved in all patients after 29 days without complications, though factors such as range of motion were not assessed and a need for a long-term follow-up with greater numbers of patients was noted. UBM scaffolds have also been applied to skeletal muscle repair[40]. Skeletal muscle repair in patients with significant muscle loss, characterized by a 25% increase in skeletal muscle volume in the area of implantation, was achieved in three out of five patients.

SIS has been applied for the repair of bone, cardiac tissue, nerves, and various soft tissues. One SIS-based augmenting material, DynaMatrix®, has demonstrated potential for relieving gingivitis by supplementing keratinized gum tissue[41]. CorMatrix®, a SIS-based cardiac patch that has been used for aortic valve replacement, has demonstrated a relatively high short-term success rate for cardiac defect repair[42,43]. While CorMatrix® has most often been implanted in children, a 90-year-old woman survived three years after aortic valve replacement, ultimately

dying of cardiac arrest unrelated to patch failure. The patch was found to have stimulated regeneration of native tissue with histology comparable to native aortic value tissue. There has been some implication of severe inflammation, though extensive evaluation of the immune response to CorMatrix® has not been performed due to limited existence of clinical studies conducted for longer than one year[42].

Materials derived from various other tissues have also been developed and clinically tested. An esophageal dECM scaffold composed of three layers – the mucosa, submucosa, and muscularis externa, the outermost layer of muscle in the esophagus – was implanted in five male patients following surgical removal of esophageal cancer to eliminate the need for esophagectomy, a procedure with high risk of complication[6,44]. All five patients were found to have regenerated, healthy epithelium and mucosa after 4-24 months, and were able to eat a normal diet, though two developed mild gastroesophageal reflux. Existing xenogeneic grafts have shown highly limited graft rejection over both traditional tissue transplants and many synthetic biomaterials. The leading theory for this phenomena is that dECM stimulates an anti-inflammatory Th-2 lymphocyte response[38].

2.3.1. Decellularization

To successfully decellularize VF, a combination of decellularization agents are generally used in sequence, to maximize the elimination of cells and immunogenic molecules while minimizing alteration of ECM organization and composition[45]. No existing method of decellularization completely circumvents ECM alteration or succeeds in removing 100% of cellular components. Therefore, ECM disruption must be limited while maximizing cell removal. Because the ECM of different tissues possess highly variable thickness, morphology, and cell and fiber density,

decellularization protocols derived for thin mucosal tissues like UBM and SIS, are insufficient for thicker, more dense materials including the whole VF[2].

While UBM and SIS can be decellularized with two hours of agitation in 0.1% peracetic acid, VF require a multi-step decellularization protocol[2,12,21]. These methods may include freeze-thaw cycles, pressure gradients, supercritical fluids, or perfusion, though the most common steps in a VF decellularization protocol are (1) ionic or non-ionic surfactant-based solubilization of DNA, lipids and cytoplasmic membranes, (2) nucleotide digestion with nuclease(s), and (3) acid solubilization of nucleic acids and cytoplasm. The selection of decellularization agents determines both the efficacy of decellularization and how much the ECM structure is altered in the process.

Three surfactants have been investigated for VF decellularization: Triton X-100, a non-ionic surfactant, and sodium dodecyl sulfate (SDS) and sodium deoxycholate, ionic surfactants[38]. All three surfactants reduce GAG content, though SDS does so most significantly, up to 50%. As a non-ionic surfactant, Triton X-100 is considered milder in action than ionic surfactants but its efficacy is debated, and it can weaken the collagen network. Decellularization with Triton X-100 alone is unsuccessful. SDS is commonly selected for use in tissue decellularization. While it is an effective detergent, it can alter the tertiary structure of structural proteins by, for example, denaturing collagen's triple helix and removing the outer layer of elastin fibers, and break bonds between ECM and growth factors. Residual SDS can also inhibit constructive remodeling and be difficult to impossible to completely remove. Although sodium deoxycholate can also alter ECM composition and cannot be used alone, short exposure times are more effective for decellularization than Triton X-100 and alters collagen organization and GAG content to a lesser

degree than SDS[46]. In combination with nuclease and acid steps, sodium deoxycholate helps find a balance between decellularization and ECM preservation[12].

Deoxyribonuclease I and ribonuclease I are highly effective in removing nucleotides from ECM, due to their specific binding to and cleavage of DNA and RNA, respectively[2]. However, nucleases may lose efficacy over time, due to the release of nuclease inhibitors from lysed cells as decellularization proceeds, requiring the replacement of enzyme solution. As previously mentioned, 0.1% peracetic acid is highly effective in solubilizing cellular material and causes less significant damage to collagen and ECM mechanical properties over short exposure times. However, it is insufficient to completely decellularize VF alone. The combination of surfactant, nuclease, and acid decellularization agents is essential to maximize the decellularization of VF while limiting their impact of ECM composition and structure. As such, optimization of ECM decellularization procedures warrants further investigation, as proposed in this thesis.

2.3.2. Whole Tissue Scaffolds in Vocal Fold Tissue Engineering

Although there are a wide variety of dECM-based scaffolds under development, two areas have received the most extensive attention for VF tissue engineering: whole dECM scaffolds, and dECM hydrogels. The first decellularized scaffold for VF tissue engineering was designed by Huber et al in 2003[47]. This scaffold consisted of four layers of UBM and was investigated as a replacement for damaged VF in canines, by surgical implantation in the place of excised VF and connected cartilage. Regeneration of the canine VF and surrounding cartilage was measured three and twelve months after implantation, revealing the growth of several tissues including the epithelium, skeletal muscle, and cartilage. However, the mechanical properties and cellular response to the scaffold were not evaluated.

Kitamura et al investigated the potential for VF regeneration in canines using a UBM scaffold created by stacking four layers of UBM with dimensions approximately the dimensions of a VF (4 cm x 4 cm), bound by dehydration under vacuum conditions[48]. Although the scaffolds showed integration of epithelial cells and a new epithelial layer after implantation in canines for one month, as well as regeneration of surrounding muscle and cartilage, the regenerated tissue exhibited fibrotic characteristics. A flaw in the study noted by the authors was that degradation kinetics were not evaluated, only the composition of the regenerated VF after six months.

A canine study was also performed in six dogs by Pitman et al where VF scaffolds derived from SIS were implanted and inflammation monitored over a period of six weeks[49]. Inflammation was comparable to a sham surgery control – peaking at four weeks but decreasing to mild levels at six weeks. Significant levels of HA were detected in the VF treated with SIS scaffolds, indicating a regenerative response, but fibrotic scarring was not observed. The authors concluded the SIS scaffold presented an improvement over existing surgical implants for VF repair.

Scaffolds derived from decellularized human, bovine, and porcine VF have also been evaluated for application in VF tissue engineering. Of the potential xenogeneic sources, porcine tissue is most similar in ECM composition to human VF[13,18], though early whole dECM scaffolds were primarily composed of bovine VF. Xu et al conducted an extensive investigation of bovine VF dECM scaffolds, decellularized in a three-agent protocol consisting of sequential exposure to high concentration sodium chloride, nucleases, and ethanol[38]. These scaffolds contained collagen retained in its native orientation, and stimulated adhesion and infiltration of human VF fibroblasts (HVFF) and new ECM deposition. While decellularization increased the elastic and viscous moduli and dynamic viscosity of scaffolds significantly above the expected range for human VF, these properties were reduced to levels comparable to human VF twenty-one days

after seeding with HVFF. Subsequent experiments showed the bovine VF dECM scaffolds possessed interconnected pores and high permeability, enabling transport of essential nutrients and cellular infiltration[50]. The *in vivo* response was evaluated in a rat model as a measure of ECM deposition and cellular infiltration. Although inflammatory cells were found within implanted VF for the first week, significant and gradually decreasing GAG and organized collagen I and III deposition was measured over three months, with the final VF void of fibrotic tissue[3]. Incorporation of hepatocyte growth factor (HGF), released from the dECM scaffold over seven days *in vitro*, limited inflammatory cell infiltration[51].

A comparison of bovine VF-derived dECM scaffolds decellularized with 1% SDS to native VF was conducted by Tse et al, as a function of viscoelastic properties, matrix composition, basement membrane protein retention and organization[52]. Significant changes in viscoelastic properties including the storage and loss moduli were not found following decellularization. Although collagen and elastin were retained, HA was significantly reduced, but could be added during cell seeding or injected separately. While these results were favourable, *in vivo* studies with dECM scaffolds for VF tissue engineering have demonstrated rapid degradation and failure to reduce fibrotic morphology.

2.3.3. dECM-Particle Based Hydrogels

Homogenizing dECM into microparticles, which can then be reconstructed as hydrogels, has been investigated as a method of overcoming the limitations of whole dECM scaffolds. Microparticles can be synthesized by a variety of methods, including manual milling with blenders or mortar and pestle, bead milling in tissue lysers, or cryomilling[45,53]. These microparticles retain the same biomolecular components as whole ECM and their corresponding nanostructure. While several methods for producing dECM hydrogels have been suggested,

solubilization with pepsin, an enzyme obtained from porcine gastric acid, is the most established protocol[37,46]. This protocol involves the suspension of dECM microparticles in pepsin in 0.1 M hydrochloric or 0.5 M acetic acid at room temperature for 24-72 hours. When the dECM microparticles are completely solubilized, the reaction is halted by neutralization to physiological pH with sodium hydroxide (NaOH). Resuspension at physiological salt concentrations and incubation at 37 ºC induces hydrogel formation.

Several studies conducted on dECM hydrogels intended for bone, cartilage, cardiovascular, gastrointestinal and nerve tissue engineering have investigated the importance of tissue source in dECM hydrogels. With one exception, the work of Keane et al, these studies concluded dECM derived from the target tissue substantially enhances the efficacy of dECM hydrogels. In the Keane study, a notable difference between the efficacy of UBM, SIS, and esophageal dECM-based hydrogels in gastrointestinal remodeling was not found *in vivo*[2]. Despite an increase in esophageal stem cell migration and organoid assembly for the esophageal dECM hydrogel *in vitro* over UBM and SIS, an enhanced cellular response was not observed in a murine model.

The efficacy of bone tissue derived dECM and various heterologous dECMs in inducing osteogenesis and regenerating bone tissue were assessed using electrospun dECM and poly (ε – caprolactone) (PCL) scaffolds[7]. Electrospinning is the deposition of fibers with micro or nano-sized diameters on a collection plate in an organized or random pattern to form a scaffold. Particles derived from bone, cartilage, lung, spleen, adipose tissues were evaluated. Bone dECM most significantly promoted osteogenesis, while dECM derived from cartilage and adipose induced a lower but still significant degree of osteogenesis. Spleen and lung dECM induced less osteogenesis than a PCL-only control. While all dECM types facilitated cell proliferation and survival, the amount of osteogenesis might be related to the composition of the tissue source.

Although mechanical differences between the hydrogels may also affect osteocyte differentiation, mechanical factors were not investigated in that study.

Similar experiments were conducted by Beachley et al for a two-layer spherical hydrogel composed of a HA-dECM center surrounded by a chondroitin sulfate-dECM shell[10]. Bone, cartilage, adipose, liver, spleen, and lung dECM were again evaluated. However, instead of solubilizing the dECM by pepsin digestion, chondroitin sulfate and HA were modified with N-hydroxysuccinimide (NHS), which triggered crosslinking with whole dECM microparticles upon mixing to fabricate the hydrogel. The efficacy of bone defect repair was evaluated in a rat bone defect model. The bone-derived dECM enhanced osteogenesis over all other types of dECM and regenerated bone within defects at levels comparable to native tissue.

A dECM hydrogel for repair of ischemic cardiac muscle, damaged by peripheral artery disease, was synthesized and injected in a rat model[54]. Two types of dECM, skeletal muscle and umbilical cord, were evaluated. Perfusion of blood through the muscle was enhanced in both types, though significantly healthier tissue morphology, greater cell survival, and blood vessel regeneration including potential arteriogenesis, were measured for the skeletal muscle dECM. The anti-inflammatory immune response generated only by the skeletal muscle dECM was the likely cause of these differences.

Hydrogels produced from SIS, bovine pericardium, and rail tail and bovine Achilles tendons were fabricated and the effect of their differences in composition on hydrogel formation, mechanics, biocompatibility, and macrophage response were investigated[5]. The goal of this study was to improve the ability of investigators to tune the properties of dECM hydrogels. The higher concentration of fibronectin, laminin, and sulfated GAGs in SIS and bovine pericardium expedited gelation and enhanced swelling, possibly due to the greater ability of collagen to

physically crosslink with these components. Greater crosslinking resulted in smaller pore size, slower degradation rates, and greater elastic moduli. Hydrogels containing greater quantities of ECM components – SIS and bovine pericardium – enhanced both biocompatibility and anti-inflammatory macrophage response. These results indicate both tissue source and the alterations in ECM content caused by decellularization enable the prediction of gelation, mechanical, and biological properties of dECM hydrogels and may be a step toward more effective tuning of their fabrication process.

The importance of dECM source has also been investigated for neural tissue engineering. As a potential method for treating spinal cord injuries, Viswanath et al investigated the impact of dECM hydrogels derived from spinal cord, dentine, and bone on mesenchymal stem cell (MSC) differentiation into neural cells[11]. The differences in ECM composition of the source were found to alter the mechanical strength and bioactive properties of the hydrogels. Spinal cord and bone hydrogels formed more quickly than dentine hydrogels, which also possessed the lowest elastic and viscous moduli. Although increased neural differentiation marker expression in MSCs was observed for spinal cord and bone dECM hydrogels, spinal cord tissue induced a more significant differentiation response in terms of marker expression and neurite morphology.

Porcine brain, spinal cord, and UBM derived dECM hydrogels were evaluated for their efficacy in regeneration of central nervous system tissue, with significant differences observed in the composition and mechanical properties of each[55]. Additionally, spinal cord and brain dECM induced more significant differentiation of neural stem cells into neurons. It should also be noted that because different tissue types require different decellularization processes, these conclusions can be thrown into doubt. As a result, the impact of tissue source on dECM hydrogel efficacy for tissue-specific applications remain ambiguous. However, the general consensus is that hydrogels

with fewer alterations in composition and structure during the decellularization process gel more efficiently and possess properties more favorable to the regeneration of healthy tissue. Prior to the material described herein, dECM hydrogels applied VF tissue engineering have been fabricated from SIS and focused on cellular and *in vivo* responses without consideration of mechanical properties.

The first dECM hydrogel for VF tissue engineering was developed by Choi et al to regenerate native VF by inducing differentiation of encapsulated MSCs[9]. To prepare the hydrogel, SIS was extracted from porcine jejunum and solubilized with 0.1% pepsin in 3% acetic acid. Neutralized and freeze-dried SIS powder was mixed with MSCs and gelation induced at 37 ºC, either by incubation *in vitro* or in rabbits *in vivo*. Encapsulation in the SIS hydrogel heightened MSC adhesion and proliferation on the scaffold and injury site in VF and resulted in decreased fibrotic scarring compared to controls treated with MSC or SIS only after eight weeks. In comparison to the controls, lower and more organized collagen deposition occurred, and HA synthesis was stimulated. These differences are indicative of a strong healing response, causing the decrease in fibrosis. Vibratory characteristics of the VF were evaluated by videokymography at the conclusion of the study, with the amplitude of vibration increased by a factor of three for the MSC-encapsulated SIS hydrogel over either control. No other mechanical property or biocompatibility experiments were performed.

Using commercial SIS powder, Huang et al developed an SIS-HA composite hydrogel that supported adhesion and differentiation of ASCs into HVFF to a greater degree than HA only or HA-collagen hydrogels[8]. The SIS-HA hydrogel consisted of 1.5 mg/mL SIS and 10 mg/mL HA after mixing. Differentiation of ASCs was evaluated by analyzing cell morphology, staining for endoglin, and measuring secretion of several growth factors and cytokines as well as deposition

of elastin, decorin, and chondroitin sulfate. Endoglin presence was lowest in the SIS-HA gel, which enhanced secretion of vascular endothelial growth factor, hepatocyte growth factor, and interleuikin-8. These growth factors and cytokines are thought to be involved in the differentiation of ASCs into HVFF. Elastin and chondroitin sulfate deposition were enhanced over both controls, while decorin deposition was approximately equivalent to the Collagen-HA gel and greater than the HA gel. The dECM gel also stimulated the differentiation of ASCs into the elongated morphology of HVFF. Bound growth factors and ECM proteins within the SIS were proposed to enhance stem cell differentiation observed in the SIS-HA gel. Mechanical evaluation; however, was not performed. Because a scaffold intended for use in VF tissue engineering must be capable of performing the mechanical function of native VF – undergoing elongation up to 30% and vibrating across the range of human vocal frequencies. Failure to evaluate the mechanical properties was a key shortcoming of these studies.

2.4. Research Gaps

In VF tissue engineering, dECM-based biomaterials remain an untapped possibility for replicating the structure of native VF. The majority of existing research has applied implantable scaffolds derived from UBM, SIS, or whole VF dECM to the regeneration of VF. Because these materials require surgery, implantation of these materials may result in an inflammatory response that negates the benefits of dECM for triggering an anti-inflammatory immune response and consequentially inhibit the constructive remodeling response. An injectable material would be favorable for limiting the potential inflammatory response. However, whole dECM cannot be injected as it is a solid scaffold that needs to be properly oriented.

While dECM hydrogels have been explored for a variety of materials, only two studies have explored dECM hydrogels for VF tissue engineering applications. These hydrogels consisted of

commercial SIS powder, a material similar but not identical in composition to VF ECM. As previously described, multiple studies in bone, cardiovascular, musculoskeletal, and nerve tissue engineering have shown that dECM source can have a significant impact on remodeling outcome. Additionally, the two studies that used SIS to produce a dECM hydrogel for VF tissue engineering did not conduct extensive evaluation of the mechanical properties of their materials, and instead focused on stem cell differentiation and preclinical animal testing. In the initial phases of biomaterial development, mechanical properties and biomaterial structure are imperative, particularly for application in organs with unique biomechanical properties such as VF. For the project described herein, the hypothesis was that a VF-derived dECM hydrogel would replicate the native mechanics of VF and provide a favorable environment for HVFF attachment and proliferation.

Chapter 3. Methodology

3.1. Materials

Adult porcine larynges were obtained from a local abattoir, Olymel S.E.C., in Montréal, Quebec. Collagen I from rat tail was obtained from Corning Inc. (NY, USA, Lot. 8204004). Hyaluronic acid sodium salt was purchased from Abcam (Cambridge, UK, Lot. GR16171-46). Sodium deoxycholate (Lot. BCBT0097), peracetic acid (Lot. BCBS6812V), DNase I (Lot. SLBT5559), Verhoeff Van Gieson Staining Kit (Lot. SBLT1512), formalin (Lot. SBR6658V), hyaluronidase, papain (Lot. SLBT1479), pepsin (Lot. SLBL6640V), N-ethylmaleimide (Lot. SLBW9248), benzamidine (Lot. BCBT9196), heparin sodium salt (Batch 2.1), urea (Lot. SLBX4778), and Phenylmethylsulphonyl Fluoride (PMSF, Lot. RT2213762) were purchased from Sigma Aldrich (St. Louis, Missouri, USA). Ribonuclease A (RNase, Lot. 14284724) from bovine pancreas was purchased from Roche Industries (Mannheim, Germany). Tris Base (Lot. 161603), sulfuric acid (Lot. 146658), ammonium hydroxide (Lot. 162522), and Pierce™ BCA Total Protein Assay (Lot. QE216982) were purchased from Fisher Scientific (QC, Canada). Dulbecco's Modified Eagle Medium and Fetal Bovine Serum were purchased from Multicell, hyaluronidase buffer and Alcian Blue 1%, pH 2.5 stain kit from Newcomer Supply (WI, USA), Bovine Serum Albumin from Bio-RAD (Cat. 500-0007), collagenase I from Worthington (NJ, USA), and sodium hydroxide from Acros Organics (NJ, USA, Lot. A0367065) Fastin® Elastin and Sircol® Total Collagen assays were obtained from Biocolor (UK) and Quant-iT™ PicoGreen® dsDNA kit (Lot. 1875966) and Live/Dead™ Cellular Viability and Cytotoxity Kit (1932445) from Invitrogen (CA, USA).

3.2 Overview of VF-dECM hydrogel fabrication process

The general workflow of VF-dECM hydrogel fabrication process includes five major steps of decellularization, homogenization, solubilization, neutralization, and gelation steps **(Figure 1)**. Specific details for each step are described in the following sections.

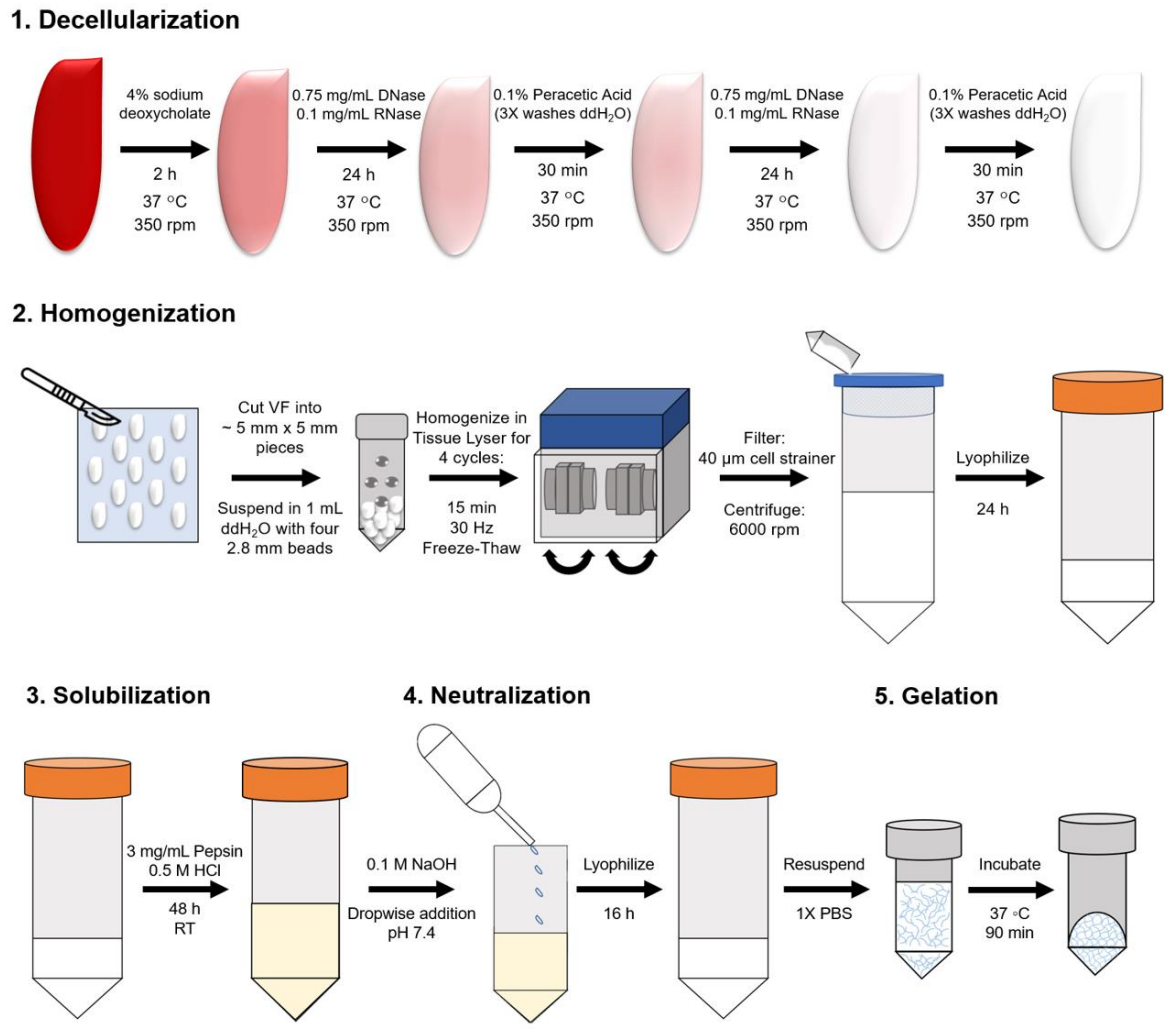

Figure 1. dECM Hydrogel Fabrication Process. (1) Decellularization: dissected porcine VF were agitated at 350 rpm (0.2 x g) in an Eppendorf ThermoMixer® C and 37 ºC in 4% sodium deoxycholate for 2 h, 273 KU DNase and 10 mg/mL RNase for 24 h, and 0.1% peracetic acid for 30 min before washing 3 times in water and repeating the nuclease and acid decellularization steps. The dECM were lyophilized for storage until homogenization **(2) Homogenization:**

dECM were cut into 5 mm x 5 mm pieces and suspended in 1 mL ddH_2O with four 2.8 mm beads and homogenized for four cycles of 15 minutes at 30 Hz in a tissue lyser, freezing the suspension at -80 ◦C and thawing between each cycle. Homogenized dECM was filtered through a 40 µm cell strainer, centrifuged at 4100 x g in an Eppendorf 5430 R centrifuge with an FA-45-48-11 rotor to remove the supernatant, and lyophilized for storage. **(3) Solubilization:** dECM microparticles were suspended in 3 mg/mL pepsin in 0.5M HCl for 48 h at room temperature **(4) Neutralization:** Solubilized dECM was brought to physiological pH (pH 7.4) by dropwise addition of 0.1 M NaOH and lyophilized again **(5) Gelation:** Gelation was induced by resuspending solubilized dECM at the desired concentration in 1X PBS on ice and incubating for 90 min at 37 ºC. Physical crosslinking occurs between fibrils of dECM to form the hydrogel.

3.3. Porcine Vocal Fold Decellularization

VF decellularization protocols investigated were derived primarily from previous work by Xu[38] and Wrona[12], with several lengths of nuclease and acid exposure tested to determine the optimal protocol. Porcine larynges were dissected to remove VF, scraping residual muscle fibers from the posterior side of the VF before placing in 1.7 mL microcentrifuge tubes for decellularization. In all tested protocols, VF with an average volume of 0.52 mL[56-61] were submerged in 1 mL 4% sodium deoxycholate for 2 h. Agitation at 350 rpm (0.2 x g) in an Eppendorf ThermoMixer® C and 37 ºC was maintained throughout each decellularization protocol. The 4% sodium deoxycholate was removed and VF washed with DIH_2O for 15 min. Eight exposure times to nuclease(s) and peracetic acid were then tested. VF were submerged in: 0.75 mg/mL DNase alone or 0.75 mg/mL DNase and 0.1 mg/mL RNase for one or two cycles of 2 h or 24 h, with each nuclease cycle followed by 30 min in 0.1% peracetic acid and three 15 min washes in water. Enzymes were replaced for the second cycles. (**Table 1** for the eight testing protocols)

Decellularized VF were lyophilized overnight in a Christ Alpha 204 LDplus Lyophilizer (MBI Lab Equipment, QC, Canada) as preparation for homogenization or for storage at -20 ºC.

Table 1. Table of Variables Tested in Each Decellularization Protocol

Decellularization Protocol	DNase Concentration (mg/mL)	RNase Concentration (mg/mL)	Total Nuclease Exposure Time (h)	Total Peracetic Acid Exposure Time (h)
A	0.75	0	2	0.5
B	0.75	0	24	1
C	0.75	0	4 (2 x 24 h)	0.5
D	0.75	0	48 (2 x 24h)	1
E	0.75	0.1	2	0.5
F	0.75	0.1	24	1
G	0.75	0.1	4 (2 x 2h)	0.5
H	0.75	0.1	48 (2 x 24h)	1

3.4. dECM-Microparticle Homogenization

A dECM-microparticle production process was developed using the bead mill production method previously used by Masaeli for cartilage tissue engineering[53] and by Smith for musculoskeletal tissue engineering[62] with significant modification necessary to adapt the process to VF, a tissue type not previously used in dECM-particle based scaffolds. Lyophilized VF-dECM was weighed and cut into approximately 5 mm x 5 mm pieces using a scalpel and placed in 2 mL round bottom screw-cap microcentrifuge tubes with 1 mL distilled water (ddH_2O). Six 1.4 mm or 4 2.8 mm ceramic beads (Omni, Germany) were then added to each tube, and tubes placed in 24-sample Tissue Lyser Adapters (Qiagen, Netherlands) and secured in a Tissue Lyser II (Qiagen). Tubes were shaken for 15 min at 30 Hz at 4 ºC four times. Between each 15-minute tissue lyser cycle, dECM was frozen at -80 ºC and thawed at 37 ºC. Homogenized dECM was

filtered through a 40 µm cell strainer (Fisher) immediately following the fourth bead milling cycle and the resulting particles centrifuged at 4100 x g for 10 minutes. Supernatant was removed and dECM microparticles were lyophilized overnight, weighed on a Sartorius QUINTIX 124 – 1S analytical balance for yield determination, and stored at -20 ºC for future use. The yield of dECM particles from each bead size was quantified by finding the percent mass of dry particles produced from one decellularized VF to the dry mass of the decellularized VF.

3.5. Hydrogel Fabrication

Hydrogels were prepared at three dECM concentrations (0.5%, 1.0%, and 1.5% dECM) using a modified pepsin-solubilization method based on published protocols[8,9,63]. To prepare hydrogels, 30 mg/mL dECM was digested with 3 mg/mL pepsin in 0.1 M hydrochloric acid for 48 h at room temperature. The reaction was halted by neutralizing the solution with dropwise addition of 0.1 M sodium hydroxide (NaOH) to pH 7.4, centrifuged at 2000 x g for 10 min, and lyophilized. Solubilized dECM was resuspended in PBS to concentrations of 0.5, 1.0, and 1.5% dECM and incubated at 37 ºC for 90 min to induce gelation.

Collagen-HA (CHA) hydrogels were used as controls for the dECM hydrogels in all mechanical property and biocompatibility experiments, as they have previously undergone extensive evaluation for VF tissue engineering applications, and were fabricated according to a previously described protocol[8,26]. In brief, chilled 1.0% HA and 1.0% collagen I were mixed at a 1:1 ratio on ice. The mixture was incubated at 37 ºC for 90 min to induce gelation.

3.6. Biochemical Analysis

3.6.1. Histological Staining

Native and decellularized VF were stained for detection of cell nuclei, collagen and elastin fibers, and hyaluronic acid (HA). For all staining protocols, samples were frozen in Optimal

Cutting Temperature Embedding Medium for Frozen Tissue Specimens (O.C.T., Fisher) in Tissue-Tek® Cryomolds® (Electron Microscopy Sciences, PA, USA) molds at -80 ºC for at least 10 min. Frozen samples were removed from molds, attached to cryostat mounts with additional O.C.T., and 8 µm sections were cut and mounted on glass slides (Fisher). Sections were fixed to slides with formalin for 1 h. Slides were moved to a staining rack, washed in water, and stained according to the following protocols and stored at -80 ºC. Imaging of all slides was performed at 10X magnification on a Zeiss AxioObserver Automated Inverted Microscope (Carl Zeiss AG, DE).

Hematoxylin and Eosin (H&E) staining was used to detect cell nuclei, framed by extracellular protein, according to an established protocol[12]. Tissue sections first placed in Hematoxylin for 4 min, followed by 15 s washes in 1% acid ethanol, 0.3% ammonia water, and 95% ethanol. Eosin staining was conducted by submersion of slides for 2 min, and slides were dehydrated by two 1 min washes in 95% ethanol, two 1 min washes in 100% ethanol. To clear ethanol, slides were submerged in xylene for 10 min, and glass slide covers attached.

Collagen and Elastin Staining was performed using the Verhoeff-Van Gieson Staining kit (Sigma)[64]. Working Elastic Stain Solution was prepared by mixing 55.5 mL Alcoholic Hematoxylin Solution (5% hematoxylin in 100% ethanol), 8.30 mL Ferric Chloride Solution (10% ferric chloride in ddH_2O), 22.2 mL Wiegert's Iodine Solution (2% Potassium Iodide, 1% iodine in ddH_2O), and 13.9 mL ddH_2O. Working Ferric Chloride Solution was prepared from 7.5 mL Ferric Chloride Solution and 92.5 mL ddH_2O. Slides were submerged in the Working Elastic Stain Solution for 10 min, rinsed in ddH_2O, and differentiated in Working Ferric Chloride Solution for approximately 3 min, or until differentiated. After rinsing in ddH_2O again, differentiation was checked under a Swift Instruments M1000-D Light Microscope (Fisher) and

when successful, rinsed in 95% alcohol. Tissue sections were stained in Van Gieson Solution (picric acid, acid fuchsin) for 3 min, rinsed in 95% alcohol, cleared with xylene, and slide covers attached.

HA staining was performed using hyaluronidase Alcian Blue staining[12]. Two sets of samples were prepared and incubated in either 0.5 mg/mL Hyaluronidase in Hyaluronidase buffer (Newcomer Supply, WI, USA) or Hyaluronidase buffer alone at 37 ºC for 2 h. All slides were rinsed in ddH_2O and submerged in 3% acetic acid for 5 min. Slides were then stained in 1% Alcian blue solution, pH 2.5, for 30 min, before rinsing again in ddH_2O, and staining in Nuclear Fast Red for 5 min. After washing in ddH_2O again, slides were dehydrated twice for 1 min in 95% ethanol, and twice for 1 min in 100% ethanol, using fresh solution each time. Clearing was performed in xylene and slide covers attached before imaging.

3.6.2. DNA Content Quantification

The efficacy of tissue decellularization does not have a single measure of success. However, the most common standards are a reduction of DNA content by greater than 95%, or less than 50 ng residual DNA per mg tissue[2,21]. Quantifying the amount of residual DNA content in decellularized VF using the Quant-iT™ PicoGreen® dsDNA kit enabled the optimal decellularization protocol to be determined. Samples were taken in triplicate from VF exposed to each decellularization protocol and native VF, weighed, and digested in 250 µg/mL papain in 1X TE Buffer (10 mM Tris-HCl, 1 mM EDTA, pH 7.5), at 60 ºC for 16 h[12]. Quant-iT™ Lambda DNA standards were prepared at concentrations of 1000, 500, 100, 10, 1, 0 ng/mL by diluting a 2 µg/mL stock solution with 1X TE. PicoGreen® Reagent was prepared at diluting stock reagent with 1X TE by a factor of 200 in a dark room, to avoid light exposure. 100 µL of each reagent and sample were added to a 96-well plate (Sarstedt, QC, Canada), followed by an equal amount

of PicoGreen® Reagent in a dark environment. The plate was wrapped in aluminum foil during transfer to a Spark 10M ultraviolent-visible (UV/vis) spectrometer (Tecan, Männedorf, Switzerland), and the fluorescence read at an emission wavelength of 520 nm. The concentrations of DNA in each sample were determined from the standard curve, and the percent of DNA reduction for each decellularization method determined by comparison to the controls.

3.6.3. Total Protein Content Quantification

The total protein content of whole and homogenized dECM was determined using the Pierce™ BCA Total Protein Assay and compared to the content of dissected porcine VF. This analysis was important as a measure of the degree of change in ECM structure caused by decellularization and homogenization, and to enabling the comparison of collagen, elastin, and hyaluronic acid content to existing standards. Bovine serum albumin (BSA) standards were prepared at concentrations between 0 and 2000 µg/mL. Lyophilized samples were sliced into smaller pieces, placed in 2 mL screwcap tubes, and weighed. Tissue (10-15 mg) was suspended in 1 mL 2M Urea buffer in 50 mM Tris-HCl containing 5 mg/mL heparin to aid in GAG extraction and 1mM PMSF, 5 mM Benzamidine and 10 mM N-ethylmaleimide. The suspension was agitated for 24 h at 4 ◦C to extract proteins, then centrifuged at 11,000 x g for 10 min at 4 ◦C. Supernatant was removed, and a second extraction performed on residual tissue. Working reagent was prepared at a ratio of 50:1 Reagent A (sodium carbonate, sodium bicarbonate, Pierce® BCA detection reagent, sodium tartrate in 0.1 N sodium hydroxide) to Reagent B (Copper(II) Sulfate). 25 µL of each standard and sample and 200 µL of the working reagent were added to 96 microwell plates in triplicate and incubated at 37 ºC for 30 min, while agitated at 350 rpm (0.2 x g). Absorbance was measured at a 562 nm emission wavelength using UV/vis. Protein concentration with respect to dry mass was determined using the standard curve.

3.6.4. Collagen Content Quantification

As the highest concentration component of VF ECM, measuring changes in total collagen content was important to gaining an understanding of the changes caused to tissue by decellularization and homogenization. Collagen content of whole and homogenized dECM was compared to that of excised porcine VF by the Sircol Collagen Assay®. Lyophilized native VF, whole dECM, and dECM microparticle samples were weighed, and placed in 2 mL round-bottom, screw-capped tubes, with 50 µL of Sircol® Fragmentation Reagent (dilute acetic acid, antimicrobial agents, surfactants, Lot. AA795) for each 1 mg tissue. Tubes were incubated for 3 h at 65ºC under 300 rpm (0.15 x g) agitation. Solubilized collagen was separated from residual tissue fragments by centrifugation at 16000 x g for 10 min. Standards were prepared containing 0, 20, 40, 60, 80, and 100 µg of Sircol® Collagen Standard (1 mg/mL denatured bovine collagen in 0.1 M acetic acid, Lot. AA802), and ddH_2O added up to 100 µL. For unknown samples, 10 µL supernatant from each tube was diluted with 90 µL ddH_2O to ensure absorbance reading was in range of the standards. 1 mL Sircol® Dye Reagent (Sirius Red) was added to each standard and sample, mixed by inversion, and agitated at 300 rpm (0.15 x g) for 30 min. Each sample was centrifuged at 16,000 x g to 10 minutes. Dye was removed, and replaced with 750 µL Sircol® Acid-Salt Wash Reagent (acetic acid, sodium chloride, surfactants) and immediately centrifuged at 16,000 x g for 10 min. All fluid was removed before addition of 1 mL Sircol® Alkali Reagent (0.5 M Sodium Hydroxide, Lot. AA519). Samples were mixed by vortexing, allowed to sit at room temperature for 10 minutes, until all dye was dispersed, and vortexed a final time before 200 µL of each sample was added to a 96 well plate in triplicate. Absorbance was measured at an emission wavelength of 550 nm using UV/vis. Collagen concentration with respect to sample

mass was determined using the standard curve and normalized with respect to the total protein content.

3.6.5. Elastin Content Quantification

Changes in elastin content were also important to quantify because elastin is necessary to the elongation and vibratory properties of VF. Elastin content was quantified using the Fastin® Elastin Assay. Samples of ~20 mg were taken in triplicate from lyophilized native VF, whole decellularized VF, and dECM microparticles, placed in 1.5 mL microcentrifuge tubes, and 750 µL of 0.25 M oxalic acid added to each. In an Eppendorf® Thermomixer, samples were incubated at 100 ºC for 1 h, then cooled to room temperature before centrifuging at 11,000 x g for 10 min. Supernatant was removed, and the incubation, cooling, and centrifugation process repeated two times. Standards of α-elastin (1 mg/mL, Lot. AA688) at concentrations of 0, 12.5, 25, 50, and 100 µg/mL were prepared. 200 µL of standards and supernatant from each round of samples were added to fresh 1.5 mL microcentrifuge tubes and mixed with 200 µL Elastin Precipitating Reagent, which consists of trichloroacetic and hydrochloric acids. Precipitation was allowed to proceed for 15 minutes, before centrifugation at 11,000 x g for 10 min. Supernatant was removed to a waste beaker, and residual liquid removed by tapping tubes against kim-wipes. 1 mL of Dye Reagent (5, 10, 15, 20-tetraphenyl-21H,24H-porphine tetrasulfonate in citrate-phosphate buffer, Lot. AA732) was added to each sample. Elastin precipitate was dispersed by vortexing and the reaction between α-elastin and dye conducted for 90 min at 350 rpm (0.2 x g) and room temperature. Tubes were once again centrifuged, and all unbound dye removed. 250 µL of Dye Dissociation Reagent (guanidine HCl and propan-1-ol, Lot. AA745), vortexed to instigate dye release, allowed to sit for ten minutes, and vortexed again. Each sample was measured by UV/Vis in triplicated by adding 75 µL of tube contents to three wells of a 96-well

plate. Absorbance was measured at 513 nm using UV/vis, and readout used to determine elastin content based on the standard curve and normalized by total protein assay results.

3.6.6. Hyaluronic Acid Content Quantification

Because HA protects against VF damage and is crucial to the regenerative response, it was necessary to quantify the effect of decellularization and homogenization on HA content. Residual HA content was characterized by Bitter and Muir's uronic acid carbazole assay, adapted for VF[28,65-67]. Assay reagent was prepared by dissolving 5 mg/mL sodium tetraborate decahydrate ($Na_2B_4O_7$-$10H_2O$) in 18.4 M concentrated sulfuric acid and cooled on ice to 0 ºC. 25 mL of water was added dropwise to 200 mL of this solution while on ice. HA stock solution was prepared in ddH_2O at 1 mg/mL, and standards prepared by serial dilution for concentrations of 1-100 µg/mL. Tissue samples from native VF, whole decellularized VF, and dECM microparticles were taken in triplicate, weighed, and digested in 150 mL per mg tissue of 0.5 mg/mL Hyaluronidase in Hyaluronidase buffer at 37 ºC for 16 h. 100 µL of samples and standards in 3.5 mL of the $Na_2B_4O_7$ solution in glass vials were heated to 100 ºC for 10 minutes for HA degradation, then cooled to 0 ºC on ice. Following addition of 100 µL of 1.25 mg/mL carbazole in 100% ethanol, solution was heated to 100 ºC to develop color, cooled, and 100 µL transferred to a 96-well plate in triplicate. Absorbance was measured at 530 nm using UV/vis. The standard curve used to determine HA content and normalized by the total protein assay. Although HA is a polysaccharide, it is typically normalized by total protein[68].

3.7. Mechanical Characterization

3.7.1. Structural Imaging

The surface structure of whole decellularized VF, dECM microparticles, and dECM hydrogels was examined using Environmental Electron Scanning Microscopy (ESEM) (FEI Quanta 450,

Fisher)[69,70]. Samples were imaged on a cold stage at approximately 614 Pa, 50% humidity, and 10 ºC without further sample preparation. ESEM was used to eliminate the impact of lyophilization and sputter-coating on tissue and hydrogel structure. Pore size in each hydrogel was measured using Fiji, an ImageJ program[50,71]. Forty pores were randomly selected across images by two independent judges who were blinded to the sample condition. The diameter of each pore was measured using the length measurement tool. Average pore size was determined based on the average diameter from both judges.

3.7.2. Rheology

Rheological measurements to characterize the gelation kinetics and viscoelastic properties of dECM hydrogels and CHA gel were performed on a TA Instrument Rheometer, Discovery Hybrid HR-2 (New Castle, DE, USA) with 20 mm diameter steel parallel-plate geometry attachment[72]. Freshly prepared, chilled 0.3 mL samples were loaded to the bottom plate and the geometry lowered to a gap of 500 µm. Samples were insulated from evaporation using a solvent trap. A temperature sweep was performed at a rate of 5 ºC/min over a range of 4-37 ºC at 1 Hz oscillation frequency and 1% oscillatory strain. Temperature was held steady at 37 ºC while maintaining all other settings for a 2 h time sweep. These measurements were used in finding the gelation time. A frequency sweep was performed over 1-10 Hz at constant temperature and strain to determine whether the viscoelastic properties of dECM hydrogels are frequency dependent. To ensure the yield stress of dECM hydrogels is not within the range experienced by VF, an amplitude sweep was performed at constant oscillatory frequency over a strain range of 1-100%.

3.7.3. Swelling Tests

Swelling tests were performed starting with lyophilized dECM and CHA gels, using a protocol modified from previous experiments[26,73]. The gels were weighed and suspended in pH 7.4 PBS

and incubated at 37 ºC at a constant agitation of 300 rpm (0.15 x g). At defined time periods of 1, 3, 7, 14, and 21 days, excess PBS was removed. Samples were weighed, and used to calculate the water content using the formula:

$$R_s = \frac{W_t - W_d}{W_d} \quad \text{(Equation 1)}$$

Where W_d is the dry mass, W_t is the mass at each time-period, and R_s is the swelling ratio. This data was used to determine the swelling kinetics of the gels.

3.8. *In Vitro* Biocompatibility Assessment

3.8.1. Viability of Human Vocal Fold Fibroblasts Encapsulated in dECM-hydrogel

An effective scaffold for tissue engineering must be capable of sustaining the survival and proliferation of cells native to the tissue. HVFF are the most abundant cell population in native VF and are important to maintain ECM homeostasis[17]. Immortalized HVFF were donated from Susan Thibeault's Lab at the University of Wisconsin-Madison[74]. HVFF were cultured in T-75 flasks in Dulbecco's Modified Eagle Medium (DMEM) media containing 0.1 M Fetal Bovine Serum (FBS) and 0.1% penicillin and streptomycin. Cells were passed using Gibco® TrypLE Express (1X) dissociation reagent at 80% confluency. HVFF at passage 9 were encapsulated within dECM and CHA 3D hydrogels. Hydrogels were prepared by resuspending dECM and CHA in DMEM to achieve twice the desired concentration of each gel on ice. Each suspension was mixed with 0.5 mL DMEM containing 1.4 million HVFF cells/mL, seeded in 24-well glass bottom well plates (Eppendorf) and incubated at 37 ºC. Following gelation for 90 min, hydrogels were covered in DMEM. Cellular viability and proliferation were determined by quantification and confocal laser scanning microscopy, at 1, 3, and 7-day intervals.

Gels were stained with the Live/Dead™ Cellular Viability and Cytotoxity Kit according to established protocols[75]. Briefly, excess DMEM was removed and hydrogels were washed in 1X PBS three times for 5 min each. In a dark room, 1.2 µL calcein AM and 4 µL propidium iodide were prepared in PBS, and 250 µL was added to gels. After 30 min incubation at room temperature, dye solution was removed carefully to minimize the disturbance of the cell-gel matrix. Gels were washed three times for 5 min each with 1X PBS. Imaging was performed on an LSM 800 confocal microscope (Zeiss).

3.8.2. Enzymatic Degradation Kinetics

One of the most significant problems with existing treatments for VF is the rapid degradation rate of biomaterials derived from ECM, making an improvement in degradation kinetics imperative to the design of improved, injectable treatments. The collagenase assay is the standard for collagen-based biomaterials because collagenases are part of the matrix metalloproteinase family responsible for the degradation of ECM[76]. This assay has been extended to dECM degradation due to the predominance of collagens in dECM composition. Dry, weighed samples were incubated with 0.05% collagenase I at 37 ºC[46,76,77]. After 3, 6, 9, and 12 hours, samples were centrifuged at 11,000 x g, washed in PBS, lyophilized, and weighed. The fractional residual mass was calculated using **Eq. 2.**

$$M_{FR} = \frac{W_{it}}{W_0} x100 \qquad \text{(Equation 2)}$$

In this formula, M_{FR} represents the fractional residual mass, W_{it} is the mass at each time point, and W_0 is the original mass. The incubation, isolation, and lyophilization process was then repeated at 24 h intervals until all samples were completely degraded.

3.9. Statistical Analysis

Each experiment was performed in triplicate, and data displayed as a mean value ± the standard error, unless otherwise noted. Because vocal folds from different porcine donors were mixed during the homogenization process, hydrogels consisted of a mixture of ECM from VF within the same batch. Two sample F-tests were performed to determine variance for each variable in comparison to the control and other variables tested. The null hypothesis was declared void for samples with unequal variance, as defined by F greater than the F critical one shot. T-tests for equal or unequal variance were performed for paired comparison if F-tests indicated significant overall group differences. Alpha values were set as 0.05. When $p < .05$, the difference between two sample sets was considered statistically significant.

Chapter 4. Results

4.1. Porcine Vocal Fold Decellularization

Staining with H&E revealed a progressive decrease in nuclei presence with increasing exposure time to DNase and an additional decrease with the addition of RNase (**Figure 2**). Nuclei remained visible in samples for all conditions (**Figure 2a-h**) except the most intensive decellularization protocol (**Figure 2i)**, which underwent two cycles of 24 hours in DNase and RNase. Increasing nuclease exposure, time appeared to increase the structural changes from native VF, as shown by the more closely networked fibers in **Figure 2b**, which underwent 2 h of only DNase exposure, to the larger gaps and broken fibers in **Figure 2d,** wherein DNase exposure time was increased to 4 h total. These changes increased for longer nuclease exposure times and the addition of RNase (**Figure 2f and h)**. Homogenization of dECM into microparticles and solubilization for hydrogel fabrication were intended to reduce the importance of these changes by reforming the ECM network.

Duration of nuclease exposure significantly affected the degree of DNA removal. Increasing the exposure time to 0.75 mg/mL DNase (Protocol D) progressively decreased DNA content, down to 0.50 ± 0.15 µg DNA per mg tissue after two cycles of 24 h, or 48 h total (**Figure 3** and **Table 2**). Compared to the native VF control, Protocol D led to a significant reduction of DNA content [95 ± 1.8 %; $t(2) = 13$, $p = 0.006$]. However, DNA content in decellularized tissue must consistently be reduced by > 95% to be considered effective.[21] To further optimize the DNA reduction, addition of 0.1 mg/mL RNase to the DNase solution were tested (Protocol H). Further reduced DNA content for each length of nuclease exposure was observed, down to 0.04 ± 0.002 µg DNA per mg tissue after 48 h total with a significant reduction of 99.6 ± 0.1% compared to the native VF control [$t(2) = 14$, $p = 0.05$]. Visual Reduction of DNA content was also observed

qualitatively to a comparable degree in H&E stained decellularized VF sections. Therefore, the decellularization protocol (Protocol H) wherein VF were exposed to DNase and RNase for a total of 48 h was selected for subsequent experiments.

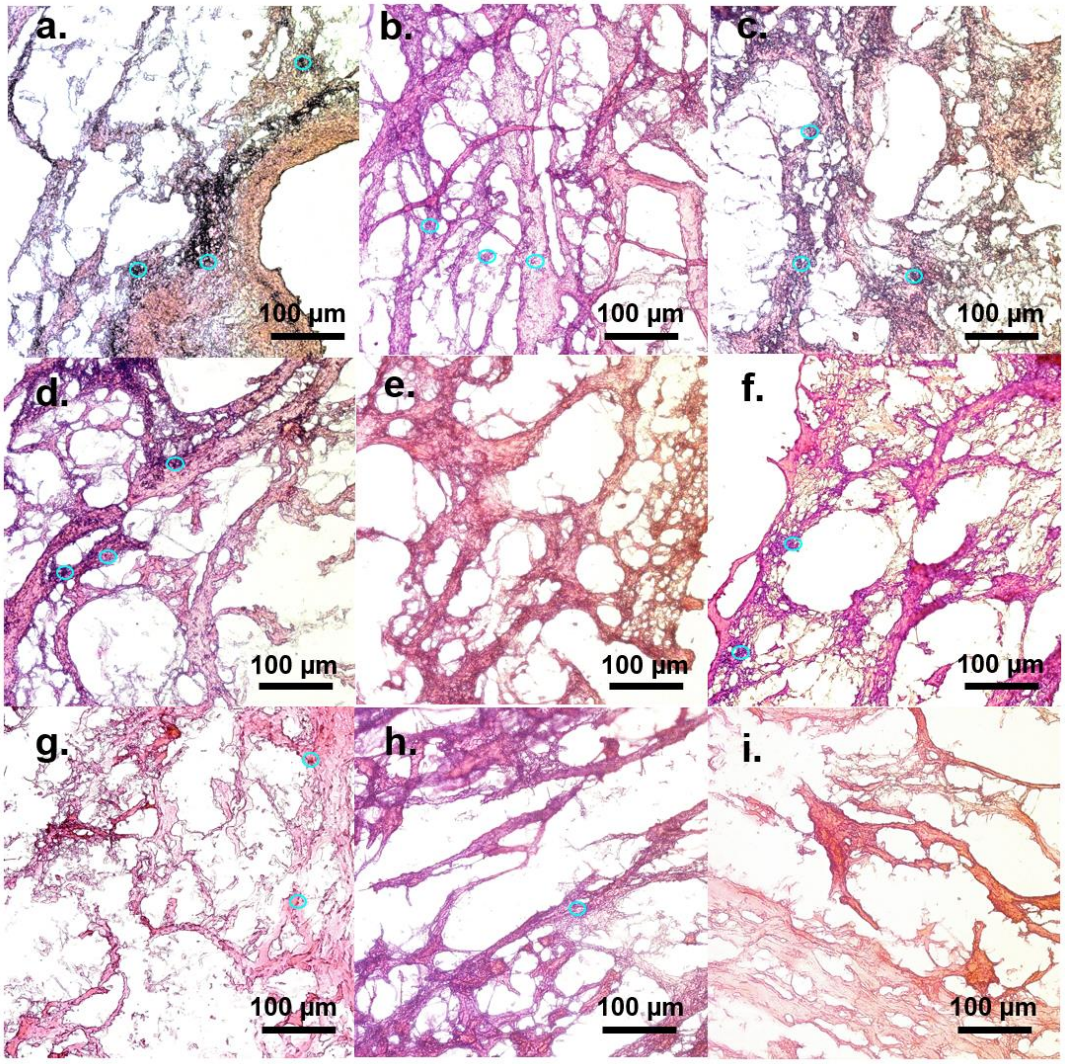

Figure 2. Histological Decellularization Results by H&E Staining (A.) Wide-field images of H&E stained 8 µm thick VF sections **(a.)** Native VF control **(b.)** 2h DNase only **(c.)** 24 h DNase only **(d.)** 2 cycles of 2 h DNase only **(e.)** 2 cycles of 24 h DNase only **(f.)** 2 h DNase + RNase **(g.)** 24 h DNase + RNase **(h.)** 2 cycles of 2 h DNase + RNase **(i.)** 2 cycles of 24 h DNase + RNase. Representative cell nuclei were circled in blue.

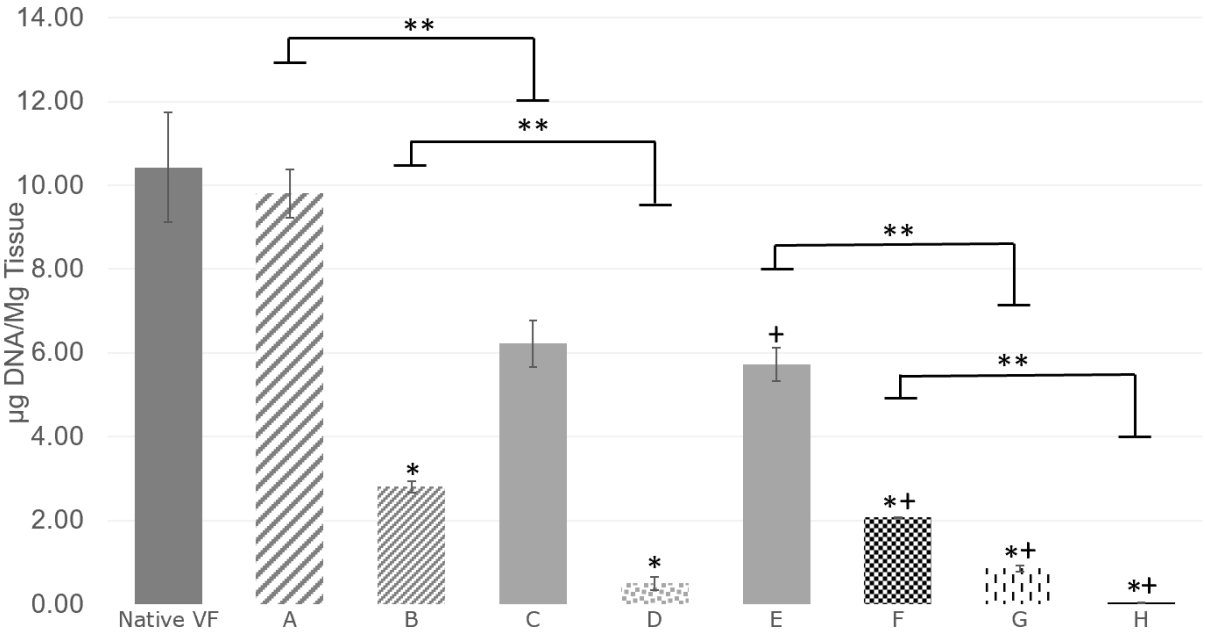

Figure 3. Quantitative Decellularization Results by DNA Removal. Plot of DNA content for the native VF control (■); 2 h DNase only (▨); 24 h DNase only (▩); 2 cycles of 2 h DNase only (▩); 2 cycles of 24 h DNase only (▩); 2 h DNase + RNase (▩); 24 h DNase + RNase (▩); 2 cycles of 2 h DNase + RNase (▩); 2 cycles of 24 h DNase + RNase (■). Statistical significance for $p < .05$, $n = 3$; (*) indicates a significant decrease in DNA content in comparison to the native VF control; (**) indicates significance in the comparison of one and two nuclease and acid cycles; (+) indicates significance in DNA content changes for the addition of RNase.

Table 2. DNA Content Quantification Data

Protocol	Sample Name	DNA Content (µg DNA/mg Tissue)	% Reduction
N/A	Native VF Control	10. ± 1.3	N/A
A	2 h DNase Exposure	9.8 ± 0.60	6.0 ± 16
B	24 h DNase Exposure	2.8 ± 0.13	73 ± 4.1
C	2 cycles of 2 h DNase	6.2 ± 0.55	40. ± 11
D	2 cycles of 24 h DNase	0.50 ± 0.15	95 ± 1.8
E	2 h DNase + RNase Exposure	5.7 ± 0.40	45 ± 9.5
F	24 h DNase + RNase Exposure	2.1 ± 0.0040	80. ± 2.2
G	2 cycles of 2 h DNase + RNase Exposure	0.85 ± 0.070	92 ± 1.5
H	2 cycles of 24 h DNase + RNase Exposure	0.040 ± 0.002	99.6 ± 0.10%

4.2. Homogenization

Progressive rounds of freeze-thawing and tissue-lyser homogenization increased the concentration of dECM microparticles in suspension. The initial sonication step loosened the binding between tissue components. Freeze-thaw cycles between rounds of homogenization would likely create microscopic gaps within the tissue sample and facilitate the breakup of dECM into particles[2]. Variation in homogenization yield was expected due to variations in VF viscoelasticity and toughness between source animals. A significant difference in the yield was observed between homogenization yield for 2.8 beads and 1.4 mm beads [$t(5) = 6.0$, $p = .002$] (**Figure 4)**. While homogenization with 2.8 mm beads consistently generated dECM microparticles with a total mass of 60. ± 8.6 % of the whole dECM, 1.4 mm beads were unable to produce particles from VF with greater elasticity or stiffness, resulting in an average yield of

9.4 ± 14 %, with one of the three samples tested yielding no particles. All subsequent homogenizations were performed using 2.8 mm ceramic beads.

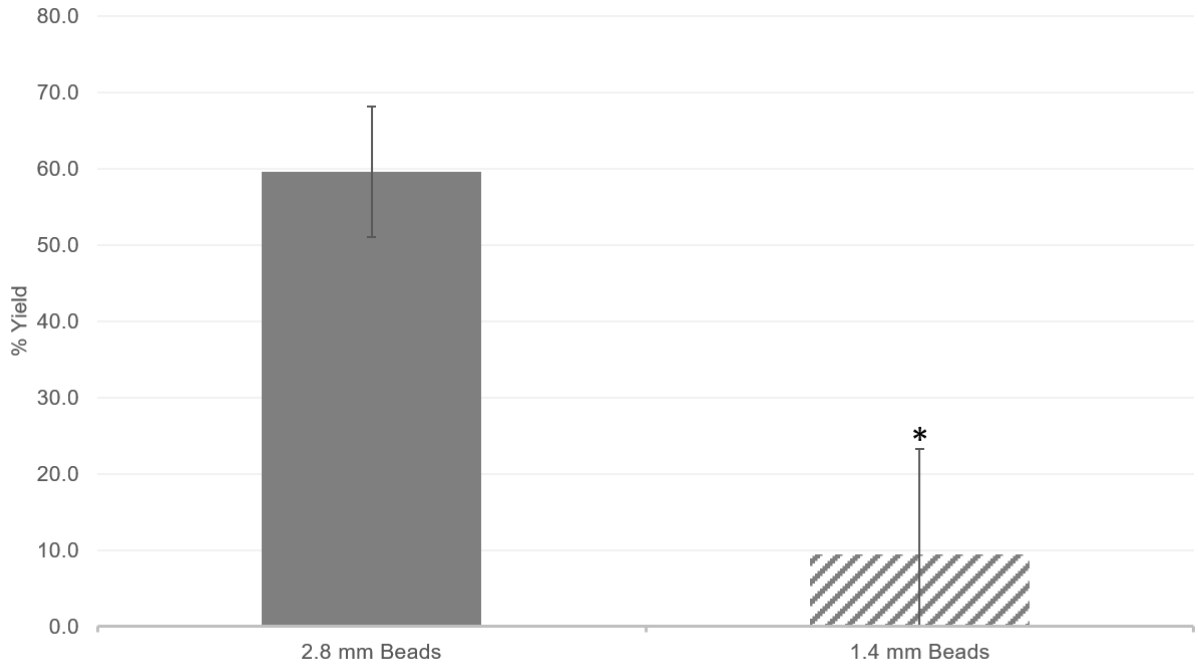

Figure 4. Homogenization yield based on total mass using 2.8 mm beads (■) and 1.4 mm beads (▨). * $p < 0.05$

4.3. Biochemical Analysis

4.3.1. Total Protein Content Quantification

The mass fraction of total protein in VF with respect to the total mass did not change significantly after decellularization. (**Table 3**) In comparison to the control, the proportion of whole dECM composed of protein appeared to decrease slightly but not statistically significant [$t(4) = 1.6$, $p = .20$]. This decrease could be attributed to sample variation. Similar insignificant differences were observed for dECM microparticles in comparison to the control [$t(4) = .61$, $p = .58$) and whole dECM ($t(4) = .94$, $p = .40$). However, this result did not indicate that no proteins, GAGs, or other molecules were lost as VF were decellularized and homogenized, only that the quantity of protein in comparison to non-protein components remained constant within

an acceptable margin of error. Biochemical analysis of total protein was necessary because the quantity of basement membrane proteins and GAGs are generally recorded as a function of total protein.

Table 3. Total Protein Content (n=3)

Sample Name	**Total Protein Content (% w/w)**
Native VF Control	91 ± 8.2
Whole dECM	83 ± 3.6
dECM Microparticles	87 ± 6.9

4.3.2. Collagen and Elastin Content Quantification

Van Gieson's staining revealed that collagen remained the primary component of the ECM following decellularization (**Figure 5)**. Collagen fibrils were dyed red-violet and created an interlocked network for cellular support in both the native VF control (**Figure 5a and c)** and decellularized tissue (**Figure 5b and d)**, through disrupted regions were visible in the network following decellularization. Regions high in elastin, dyed purple black, endured following decellularization, though possible changes in structural organization including clumping and fragmentation were noted in the decellularized whole VF (**Figure 5d)** compared to the control (**Figure 5c**).

Collagen content did not change significantly by decellularization or homogenization based on the results of the Sircol® Total Collagen Assay. In native human VF, collagens comprise 40-50% of total protein, including cells and approximately 50% of native porcine VF lamina propria[18]. The collagen assay was performed for the whole VF, not solely the lamina propria, and higher collagen concentrations are found deeper in VF tissue. On average, the native porcine VF

contained 58 ± 15 (w/w) % collagen, normalized to percent mass of total protein (**Figure 6A)**. While percent collagen appeared to increase compared to the control in decellularized whole VF to 69 ± 13 % [t(4) = .91, p = .41] and homogenized tissue to 65 ± 13 % [t(4) = .60, p = .58], these changes were not statistically significant. Alterations in percent collagen were also statistically insignificant between decellularized and homogenized dECM [t(4) = .36 p = .74]. Variation in collagen content as a result of gender, age, health and other factors are known to occur in both human and porcine VF[14], and these variables were not controlled for the porcine larynges obtained from the abattoir, accounting for the standard errors.

Elastin content was not reduced by decellularization, though a significant decrease was observed in homogenized tissue (**Figure 6B**). The percent mass of elastin of total protein in whole VF, 6.9 ± 0.58 %, and dECM, 6.4 ± 0.63 % were equivalent within an acceptable margin of error [t(4) = .97, p = .39]. Existing literature reported that the elastin content of both human and porcine VF varies between 6-10% [68]. Overall, the elastin content of VF dECM was retained after decellularization. However, a significant decrease of elastin content was found following homogenization into dECM microparticles (4.6 ± 0.48 %) in comparison to both whole VF [t(4) = 3.7, p = .02] and whole dECM [t(4) = 4.8, p = .009]. This decrease could not be ascribed to random chance or source variation, as the changes reduced elastin content below the lower limit of porcine VF. Instead, the homogenization process may have disrupted elastin crosslinking or broken elastin chains, resulting in a decrease in total elastin content[32].

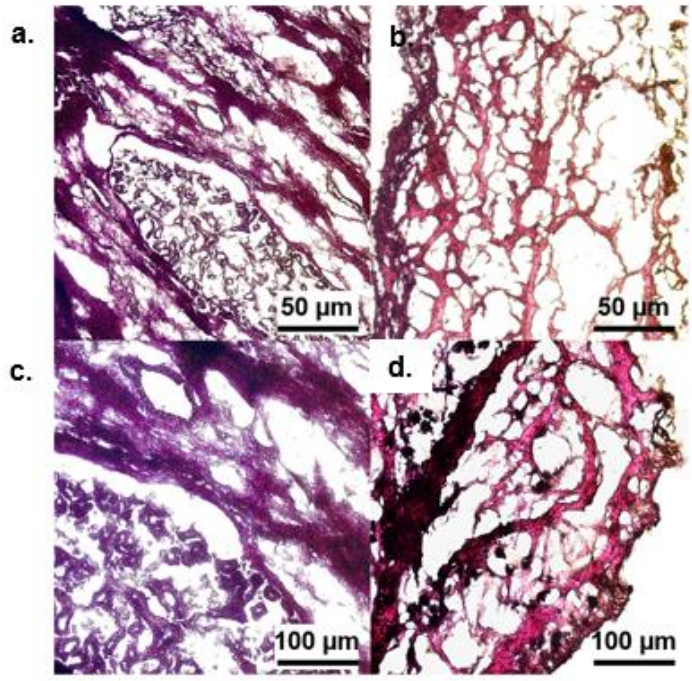

Figure 5. Histological Collagen and Elastin Retention. Van Gieson's Staining on **(a,c)** Native VF Control and **(b,d)** dECM exposed to DNase and RNase for 48 h. Collagen fibrils were stained red-violet, and elastin a darker purple-black.

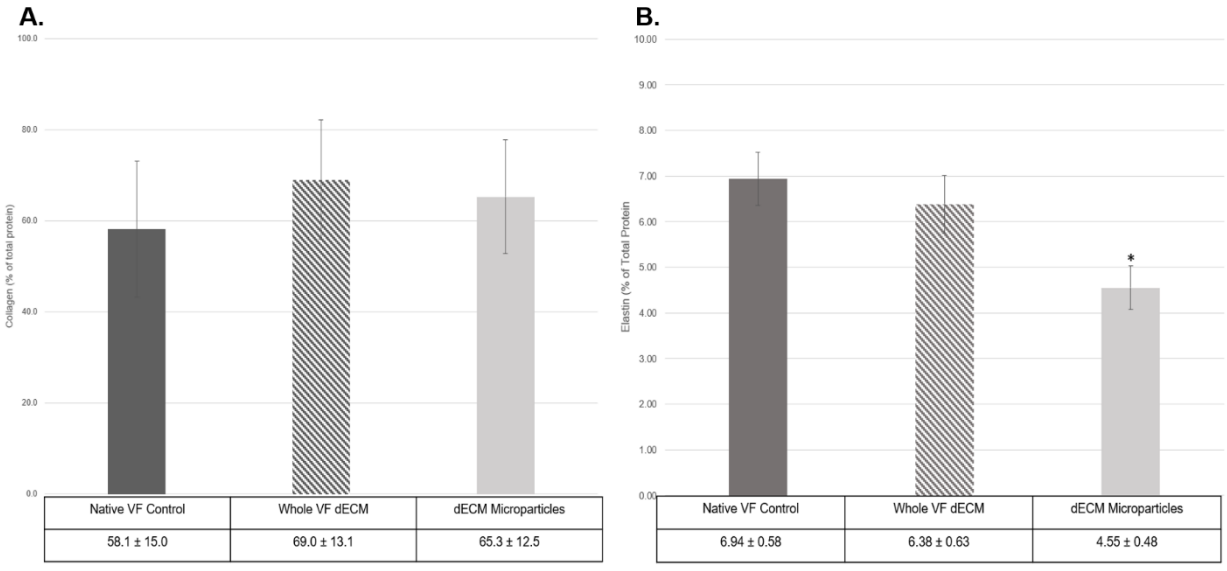

Figure 6. Quantitative Collagen and Elastin Retention. (A.) Total Collagen Content of (■) Native VF Control (■) Whole dECM (■) dECM microparticles; n=3 **(B.)** Total Elastin Content

of (■) Native VF Control (■) Whole dECM (■) dECM microparticles; n=3; Statistical significance (*) noted for $p < .05$ compared to both native VF control and whole dECM.

4.3.3. Hyaluronic Acid Content Quantification

A significant reduction in HA content was observed following both decellularization and homogenization. When stained with Alcian blue (**Figure 7A**), HA is dyed dark blue. Regions of HA were markedly more prominent in native VF at 20X magnification (**Figure 7Ac**) compared to whole dECM (**Figure 7Ad**). When treated with hyaluronidase buffer **(Figure 7Aa and 7Ab)**, the absence of staining indicated HA was removed, confirming the presence of HA in the tissue. The native VF exhibited clusters of HA throughout the tissue, while dECM showed both reduced range of HA and a lesser degree of dye attachment. Qualitative analysis therefore indicated a significant reduction in HA content, which was confirmed by the quantitative carboxyl assay.

HA content in the native porcine VF, 0.72 ± 0.12 % of the total protein (**Figure 7B**), was lower than previously reported values of 2-2.5% of the porcine VF lamina propria, and more comparable to human VF, which contains approximately 0.8% HA in the lamina propria[68]. It should be noted that hyaluronidase may degrade chondroitins as well as HA, though at a slower rate[78], which may result in imprecise results in the carboxyl assay. When compared to the results for whole decellularized tissue and dECM microparticles, a significant decrease in HA content was nonetheless apparent. This decrease was expected as decellularization using surfactants, including sodium deoxycholate, has been reported to reduce GAG content by up 50%. The reduction in HA observed in this study was even more significant. Following decellularization, HA content in whole VF dECM was 0.18 ± 0.0036 % of total protein, which was a significant reduction of 75.00 ± 4.00 % compared to the native VF control [$t(2) = 8.06$, $p = .015$]. Homogenization of the dECM to microparticles further reduced HA content to 0.10 ± 0.011 % of

total protein [t(4) = 11.69, p = .00031], which was also a significant reduction of 86.11 ± 3.29 %from the native VF [t(2) = 9.14, p = 0.012]. Although this reduction is not favorable for VF tissue engineering, HA could be replaced by a secondary injection of commercially available HA products to improve the initial biological response to the scaffold or added to the fabrication process.

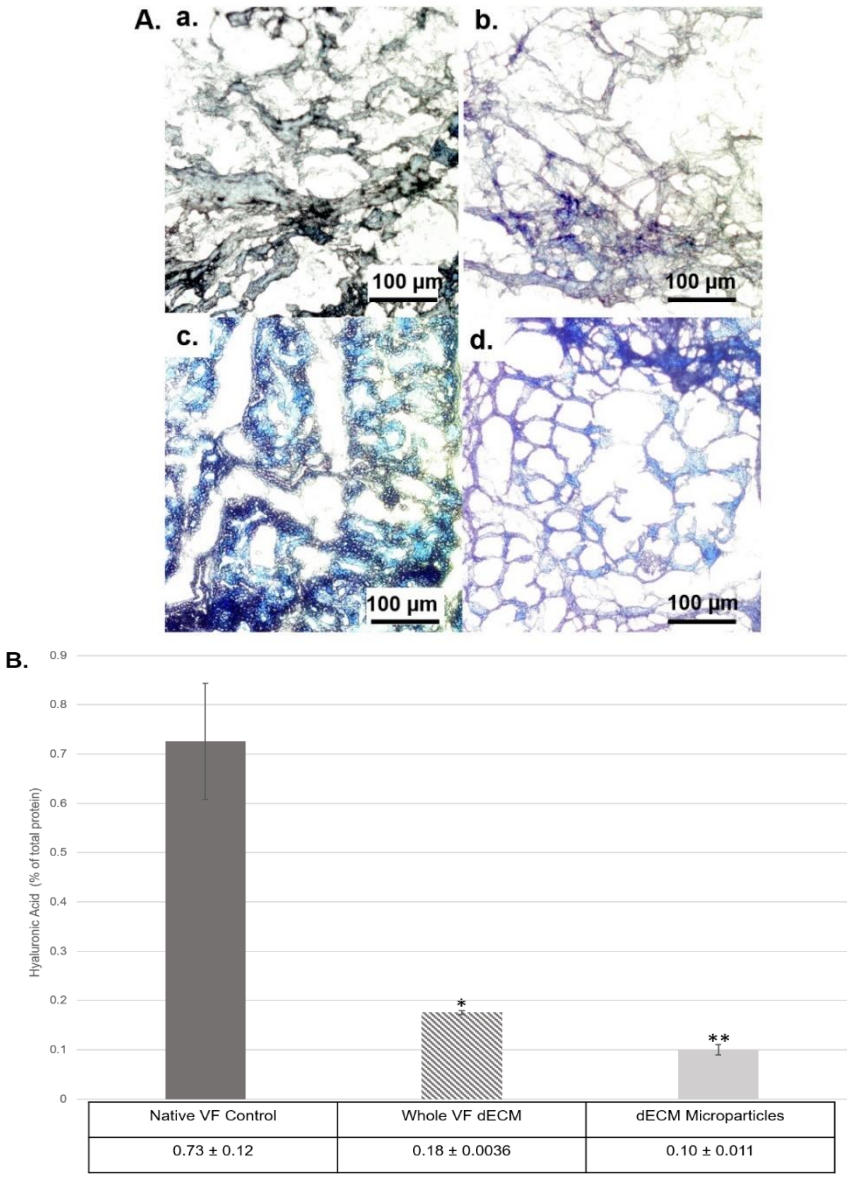

Figure 7. Histological and Quantitative HA Retention (**A.)** Alcian Blue Staining on **(a,c)** Native VF Control and **(b,d)** dECM exposed to DNase and RNase for 48 h. Dark blue regions indicate the presence of HA; **(B.)** Total HA Content of (■) Native VF Control (■) Whole dECM

(■) dECM microparticles. Statistical significance noted for $p < .05$ in relation to the native VF control (*) and both native VF control and whole dECM (**).

4.4. Mechanical Characterization

4.4.1. Structural Imaging

The overall goal of developing the dECM hydrogels proposed herein was to replicate the structure and function of VF ECM. Structurally, the ideal dECM hydrogel would resemble the whole dECM network under ESEM. The whole dECM (**Figure 8Aa**) displayed a fibrous network of proteins typical of ECM, complete with pores left behind by cells, lipids, and other biomolecules removed during decellularization. The average pore size in the whole dECM was 57 ± 26 μm, determined from an average of 40 randomly selected pores measured by two independent judges using ImageJ (**Figure 8B**). These measurements are consistent with the previously reported values for a bovine VF dECM scaffold, wherein greater than 60% of pores were within the range 10-100 μm[50].

After homogenization and filtration through the 40 μm mesh cell strainer, the dECM microparticles (**Figure 8Ab**) were immediately transported to the ESEM facility and imaged on the cold stage. Microparticle morphology resembled rounded, approximately spherical segments of ECM fiber. As expected after filtration, no dECM microparticles exceeded 40 μm in size. The diameter of forty randomly selected particles was measured, and used to determine the average dECM microparticle size, 7.4 ± 3.3 μm.

When manipulating the hydrogels, the 1.5% dECM gel exhibited the greatest structural integrity, and the 0.5% gel the least. At increasing concentrations, pores in the dECM hydrogels were more clearly defined, possibly indicating greater consistency in gelation. The 0.5% dECM (**Figure**

8Ac-d) showed evidence of a fibrous composition, indicating that dECM microparticles underwent fibrillogenesis, and physically entangled to produce the hydrogel. However, few defined pores were evident, and heterogeneous regions indicated a possible failure of all particles to fully integrate into the hydrogel. When the concentration of dECM was increased to 1.0% (**Figure 8Ae-f**), unintegrated dECM particles were visible on the surface, though the fibrilized microparticles that comprised the hydrogel appeared more cohesively intertwined. In the 1.5% dECM hydrogel (**Figure 8Ag-h**), all microparticles appeared to be integrated into the gel structure, possibly facilitating the formation of more clearly defined nano and micropores. This could explain the greater structural integrity exhibited by higher concentration dECM hydrogels. The collagen-HA (CHA) control (**Figure 8Ai-j)**, showed a uniform surface with no visible pores, as expected. Although the primary purpose of cold stage ESEM is to examine the surface structure of biomaterials such as hydrogels without the potential structural changes caused by lyophilization and sputter coating, such as pore enlargement, by maintaining a humid environment, making it useful for imaging tissues[79], this limits its applicability to homogeneous hydrogels such as collagen which resemble a smooth surface without lyophilization.

In all dECM hydrogel samples, pore diameter did not exceed 25 μm. The average pore size, calculated from 40 pores measured using ImageJ, was 1.4 ± 0.60 μm for the 0.5% dECM hydrogel, 3.4 ± 2.6 μm for the 1.0% dECM hydrogel, and 3.1 ± 0.87 μm for the 1.5% dECM hydrogel. Comparing the 0.5% dECM hydrogel with the 1.0% dECM [$t(112) = 4.3$, $p < .001$], and 1.5% dECM [$t(113) = 4.5$, $p < .001$] hydrogels suggested that an increase in average pore size occurred up to 1.0% dECM. However, the pore size of 1.0% and 1.5% dECM hydrogels were not statistically different [$t(147) = 4.27$, $p = .447$]. It is possible the greater resolution achieved on pores in the 1.5% dECM hydrogels was a result of experimental error. When

compared to the whole dECM average pore size, all three concentrations were significantly decreased [$p < 0.001$].

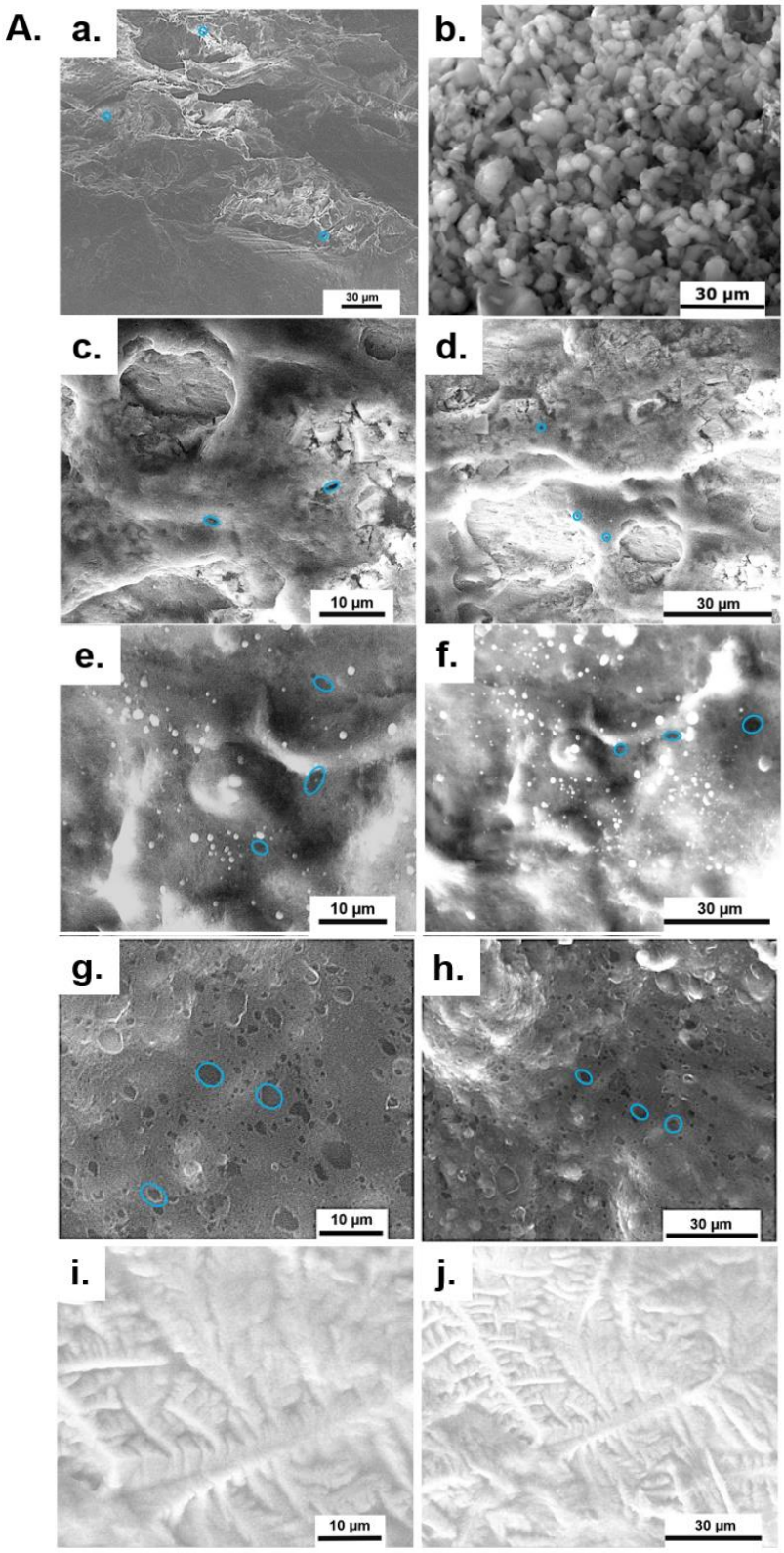

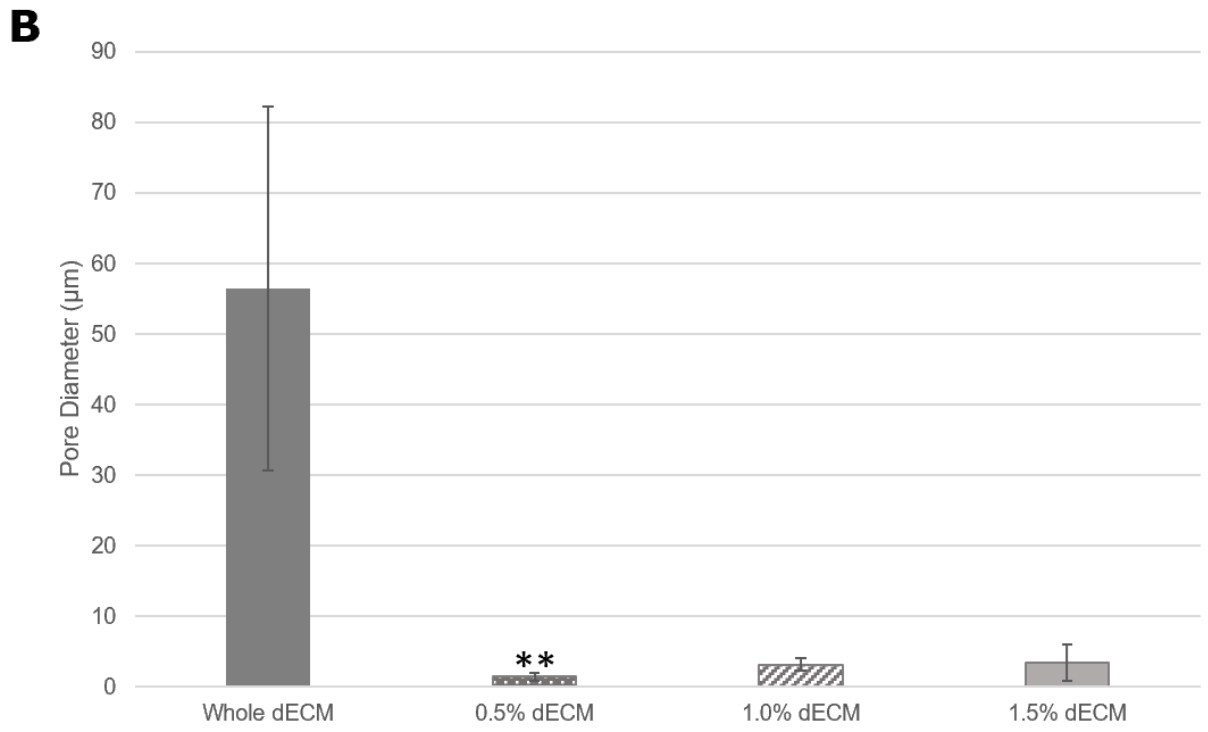

Figure 8. Environmental Scanning Electron Microscopy (ESEM) Imaging of Hydrogel Surface Characteristics and Porosity. Imaging was performed on a cold stage at 10 ◦C, 50% humidity, and 614 Pa. (A.) Representative ESEM images of (a.) a whole dECM cross-section, (b.) dECM microparticles imaged immediately after homogenization, (c-d.) 0.5% dECM hydrogel, (e-f.) 1.0% dECM hydrogel (g-h.), 1.5% dECM hydrogel, and (i-j.) CHA hydrogel. Representative examples of pores are encircled in blue. (B.) Average pore diameter determined from a random selection of at least n = 40 pores by two independent judges for (■) whole dECM, (▩) 0.5% dECM, (▨) 1.0% dECM, (▩) 1.5% dECM. (*) indicates the statistical difference of pore diameter between whole dECM and dECM hydrogels; (**) indicates statistical significance in the 0.5% dECM hydrogel pore size from 1.0% and 1.5% dECM hydrogel pore size.

4.4.2. Temperature Dependent Viscoelastic Behavior of dECM Pre-Gels

Pre-gels of dECM and CHA showed varying degrees of temperature dependence when quickly heated from 4 ºC to 37 ºC after resuspension or mixing on ice, respectively. The storage modulus (G') of the control CHA pre-gels decreased by an order of magnitude, at a rate of 1 Pa for approximately every 0.30 ºC. As the temperature approached physiological temperature, the rate at which the storage modulus decreased slowed (**Figure 9)**. The loss modulus (G") also decreased, at a rate of 1 Pa for approximately every 2 ºC.

In contrast, the dECM gels showed a lesser degree of temperature dependence in their elastic and viscous moduli, with changes dependent of dECM concentration. At 0.5% dECM, the decrease in storage and loss moduli was small, with G' decreasing by 1 Pa for every increase of 7 ºC. G" decreased at an estimated rate of only 1 Pa for 13 ◦C. The 1.0% dECM pre-gel experienced a larger decrease in G' and G" as temperature increased. A decrease of approximately 1 Pa occurred every 1.8 ºC increase for G' and every 5.0 ◦C for G". For the 1.5% dECM pre-gel, G' and G" decreased at a greater rate, though not to the same degree as the CHA pre-gel. Approximately a 1 Pa decrease in G' occurred for every 0.57 ºC, and in G" every 2.5 ºC. This indicated that the temperature-dependent behavior of the dECM pre-gels more closely resembled that of CHA as dECM concentration increased.

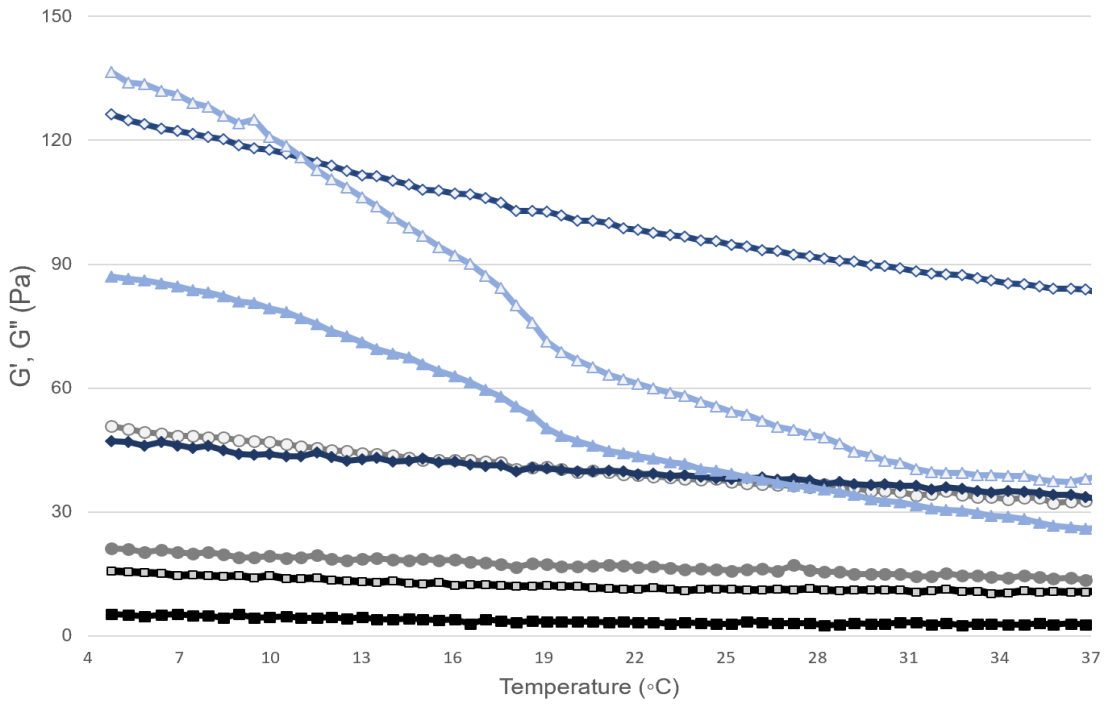

Figure 9. Temperature-Dependent Viscoelastic Behavior of dECM Pre-Gels. 0.5% dECM G' (□); 0.5% dECM G" (■); 1.0% dECM G' (⬭); 1.0% dECM G" (●); 1.5% dECM G' (◇); 1.5% dECM G" (◆); CHA G' (▲); CHA G" (△). N=3.

4.4.3. Time-Dependent Gelation Kinetics of dECM Hydrogels

Monitoring G' and G" over a period of two hours at 37 ºC from the start of hydrogel gelation enabled an estimate of required gelation time to be made for the dECM hydrogels as an injectable material. (**Figure 10**) Across the entire time sweep, G' was greater than G", indicating the biomaterial could be considered principally elastic[80]. G' of the CHA hydrogel increased steadily across the first twenty minutes, indicating that the material began acting more like an elastic solid, and stored more energy, before stabilizing. Over the same period, G" increased slightly before leveling out, indicating the CHA hydrogel began dissipating more energy as gelation occurred.

Similar behavior was observed for the 1.5% dECM hydrogel, with some differences from the CHA control. Gelation occurred over a longer period, with G' beginning to increase after approximately 5 min at physiological temperature. As G' stabilized after about one hour, this time window was considered the gelation time. Over the same time period, G" showed minimal evidence of change, signifying gelation had little impact on energy dissipation form the 1.5% dECM hydrogel. After gelation, the 1.5% dECM hydrogel fell into the lower end of the possible range of human VF storage moduli, 0.1-1 kPa[15], as did the CHA control.

When the concentration of dECM was reduced to 1.0%, the storage modulus decreased by approximately 100 Pa, yet exhibited similar gelation kinetics to the 1.5% dECM hydrogel. Over one hour, G' increased as gelation occurred, though a slower increase in G' was observed up to 2 h. Like the loss modulus of the 1.5% dECM hydrogel, G" of the 1.0% dECM hydrogel showed minimal impact on the degree of energy dissipation. However, G' of the 1.0% dECM hydrogel was below the acceptable range for human VF[15].

Although G' was greater than G" for the 0.5% dECM hydrogel, an equivalent degree of gelation was not found, despite visual observation of gelation during other studies. The slight decrease in G' for the 0.5% dECM hydrogel contradicted this observation and was observed in all three samples tested. G" of the 0.5% dECM hydrogel remained steady across the 2 h time sweep. Potential reasons for this inconsistency include that the surface area of the rheometer platform was relatively too large for sufficient physical crosslinking to occur between dECM microparticles at the low 0.5% dECM concentration or that the material formed by the 0.5% dECM during incubation did not possess the viscoelastic characteristics necessary to be considered a hydrogel. Results suggested that a 0.5% dECM hydrogel would not form a suitable

material for VF tissue engineering and calls into question the ability of VF dECM to form a gel at this concentration.

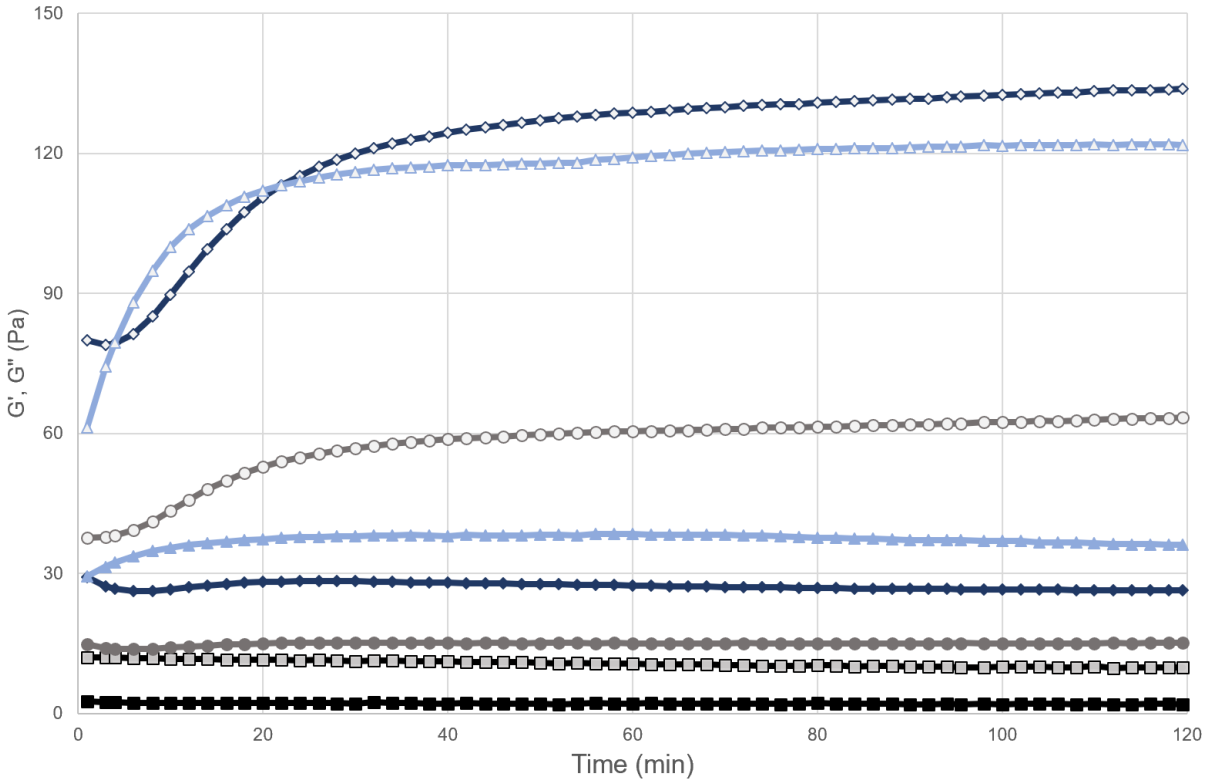

Figure 10. Time-Dependent Gelation Kinetics of dECM Hydrogels. 0.5% dECM G' (□); 0.5% dECM G" (■); 1.0% dECM G' (○); 1.0% dECM G" (●); 1.5% dECM G' (◇); 1.5% dECM G" (◆); CHA G' (▲); CHA G" (△). N=3.

4.4.4. Frequency-Dependent Viscoelastic Behavior of dECM Hydrogels

Completely gelled dECM hydrogels were exposed to frequencies from 0.01-10 Hz, to determine whether the viscoelastic behavior of the hydrogels was dependent on frequency. Direct correlation of G' and G" with frequency was observed for all three concentrations of dECM, and the CHA hydrogel, though the extent to which frequency affected viscoelasticity varied. Although G' of the CHA hydrogel initially increased steadily as frequency increased, a sharp

drop in magnitude was consistently observed as the frequency approached 10 Hz (**Figure 11**). Ultimately, G' dropped below G", indicating a loss in gel integrity. Over 0.01-10 Hz, G' and G" of native human VF generally increase linearly[81]. While frequency sweeps on linear shear rheometers, such as the TA instruments rheometer used in this study, can be unreliable above 10 Hz due to experimental artifacts related to instrument inertia[82], the low frequency at which this drop occurred indicated the CHA hydrogel would lose mechanical integrity under the higher frequency vibrations required for a VF biomaterial (60-1000 Hz).

Both the 1.5% and 1.0% dECM hydrogels demonstrated an increase of G' and G" in an approximately linear fashion as frequency increased (**Figure 11**). G' and G" of human VF also behave linearly across frequencies of 1-10 Hz. This result was consistent with the behavior of native VF across the tested frequencies, though only the 1.5% dECM hydrogel exhibited G' above 100 Pa, consistent with native VF[15,81,83]. The 0.5% dECM hydrogel demonstrated a more parabolic increase in G' and G", incompatible with native VF.

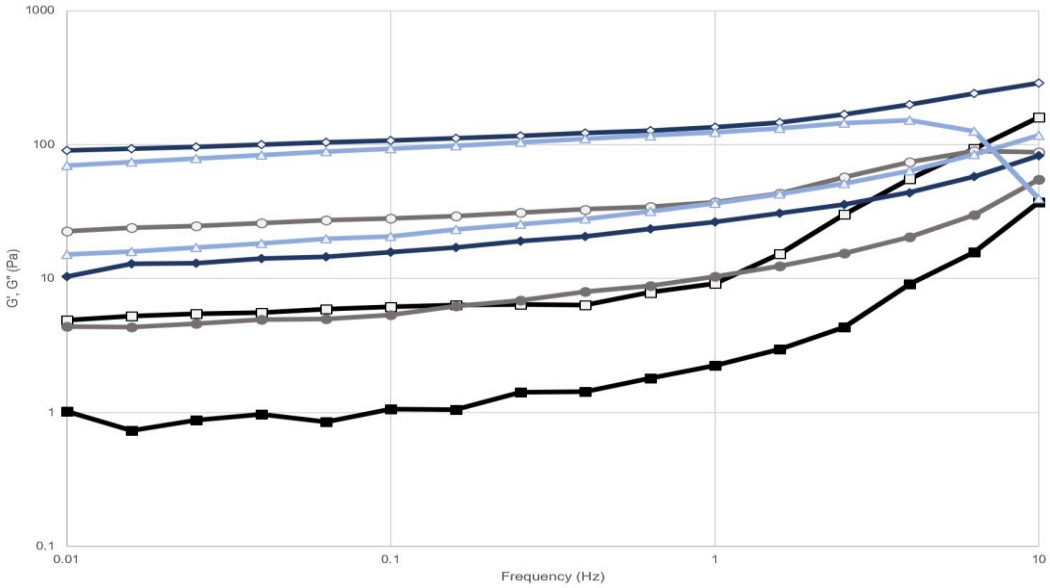

Figure 11. Frequency-Dependent Viscoelastic Behavior of dECM Hydrogels. 0.5% dECM G' (□); 0.5% dECM G" (■); 1.0% dECM G' (○); 1.0% dECM G" (●); 1.5% dECM G' (◇); 1.5% dECM G" (◆); CHA G' (▲); CHA G" (△). N=3.

4.4.5. Oscillation Amplitude-Dependent Behavior of dECM Hydrogels

Amplitude sweeps were used to determine the yield stress, at which the dECM and CHA hydrogels reached a critical point between their solid and fluid states[84]. The CHA hydrogel maintained an approximately constant G' up to 6.3% strain, before beginning to decrease (**Figure 12**). The strain at which G' and G" crossed was the yield stress, or 20 ± 4.7% for the CHA hydrogel. Above the yield stress, a deformed material is generally unable to recover its original dimensions and mechanical properties. The yield stress for CHA was lower than for any of the three dECM concentrations, all of which were on average above the deformation limit of native VF, 30% strain[24].

The 1.5% dECM hydrogel experienced its yield stress at 45 ± 7.3% strain, above the aforesaid 30% deformation limit of native VF, and significantly higher than the CHA hydrogel [$t(3) = 3.3$, $p = .044$]. Its linear, viscoelastic region also extended up to approximately 13% strain, nearly twice the linear region of the CHA control. Yield stress is the lowest value of stress or strain that causes permanent deformation of the material. The average yield stress of the 1.0% dECM hydrogel was lower, 30. ± 8.5%, though its average was not significantly different from either the 1.5% dECM hydrogel [$t(3) = 2.0$, $p = .13$], or the CHA hydrogel [$t(3) = .75$, $p = .50$]. Notably, the linear region for the 1.0% dECM hydrogel only extended to approximately 6.3%, similar to the CHA hydrogel. Although the average yield stress of the 1.0% dECM hydrogel is comparable to the deformation limit of native VF, it cannot be assumed to consistently withstand 30% strain.

Although the yield stress of the 0.5% dECM hydrogel was highest, at 59 ± 7.5% (**Table 5**), this average was not significantly different from the yield stress of the 1.5% dECM hydrogel [$t(4) = 2.0$, $p = .13$]. The linear, viscoelastic region of the 0.5% dECM hydrogel also extended up to approximately 12.5% strain. Considering the low G' value throughout the rheology experiments

for this concentration, the 0.5% dECM hydrogel did not possess the required mechanical properties to function as a regenerative scaffold for VF tissue engineering.

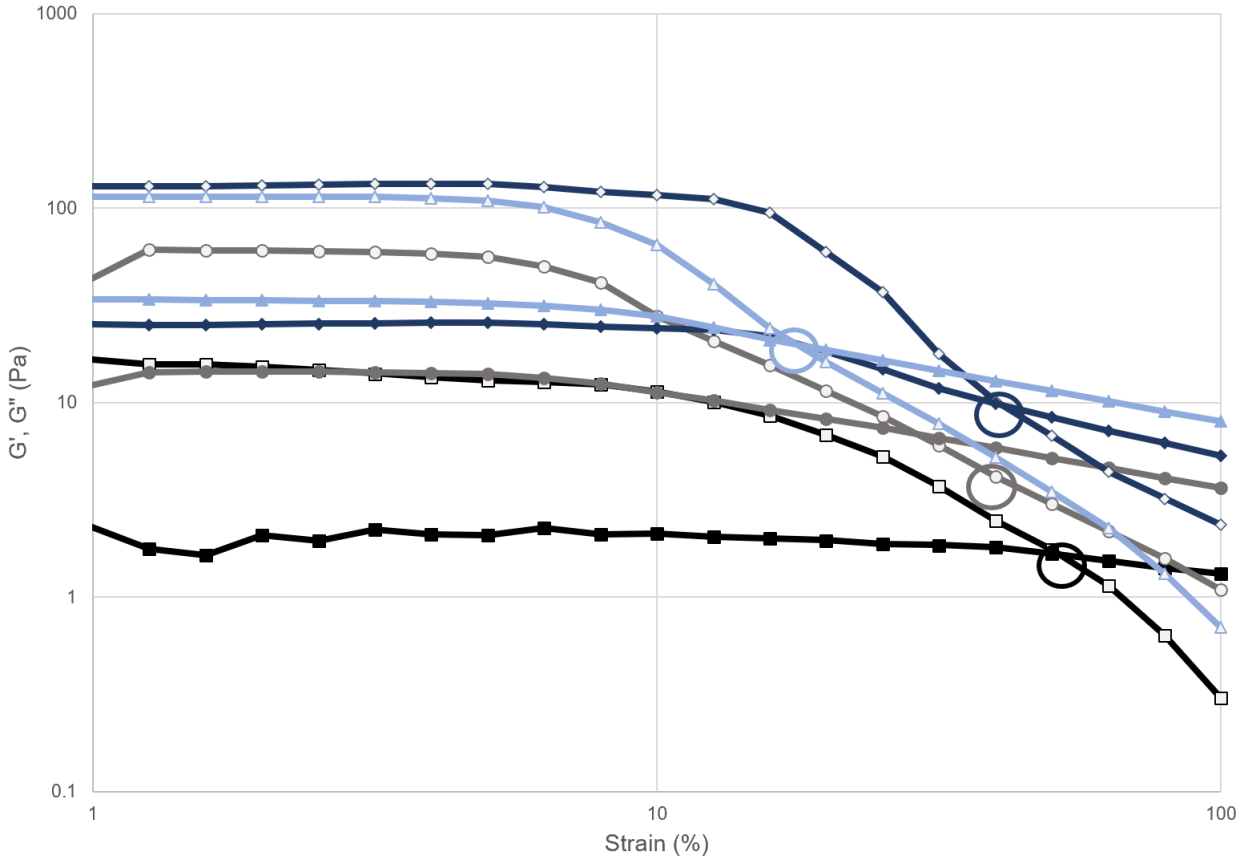

Figure 12. Yield Stress and Oscillation Amplitude-Dependent Viscoelastic Behavior of dECM Hydrogels. 0.5% dECM G' (□); 0.5% dECM G" (■); 1.0% dECM G' (○); 1.0% dECM G" (●); 1.5% dECM G' (◇); 1.5% dECM G" (◆); CHA G' (△); CHA G" (▲). The yield stress for each condition was circled; N=3.

Table 5. Yield stress of Hydrogels from Amplitude Sweep.

Condition	**Yield Stress (%)**
0.5% dECM	59 ± 7.5
1.0% dECM	30. ± 8.5
1.5% dECM	45 ± 7.3
CHA	20. ± 4.7

4.4.6. Swelling Tests

All three dECM hydrogels and the CHA control reached their maximum swelling ratios after 24 h incubation in PBS. The 0.5% dECM hydrogel swelled to 2.5 ± 0.31 times of its dry mass (**Figure 13** and **Table 4**), comparable to the swelling ratio of the CHA control, 2.8 ± 0.33 [$t(4) = 1.1$, $p = .33$]. Interestingly, the higher concentration dECM hydrogels swelled to a significantly higher degree than that of CHA. The 1.0% and 1.5% dECM gels reached 4.0 ± 0.35 and 4.4 ± 0.14 times their dry mass, respectively. The difference in average swelling ratio between the two hydrogels was insignificant [$t(4) = 1.5$, $p = 0.20$]. In comparison to the CHA control, both the 1.0% dECM [$t(4) = 4.4$, $p = 0.012$] and 1.5% dECM [$t(4) = 7.5$, $p = 0.0017$] hydrogels' swelling ratios were significantly increased.

Gel retraction of statistical significance from day 1 was first observed on day 7 for all gels. The CHA hydrogel retracted by approximately 24% [$t(4) = 3.9$, $p = 0.018$], to 2.2 ± 0.27 times the dry mass on day 7. The 0.5% dECM gel contracted to a swelling ratio of 1.6 ± 0.31 times the dry mass on day 7, a retraction of approximately 37% [$t(4) = 3.7$, $p = 0.021$] from day 1. The difference in average swelling ratio between these two gels remained statistically insignificant [$t(4) = 2.7$, $p = 0.057$]. The 1.0% dECM hydrogel contracted by 10%, to 2.8 ± 0.41 times the dry

mass, becoming comparable to the swelling ratio of the CHA hydrogel [$t(4) = 2.5$, $p = 0.07$]. The 1.5% dECM hydrogel remained swollen to a higher degree than the other three gels after 7 days. It retracted by approximately 18% [$t(4) = 4.4$, $p = .012$], to 3.6 ± 0.28 times the dry mass, significantly higher than the control [$t(4) = 7.5$, $p = .0017$].

By day 21, the 0.5% dECM gel retracted to the greatest degree, by approximately 95% [$t(2) = 13$, $p = .005$] to 0.12 ± 0.03 times the dry weight. This retraction was significantly greater than that of the CHA control [$t(4) = 28$, $p < 0.0001$], which contracted by approximately 68% [$t(2) = 9.9$, $p = .010$] to 0.91 ± 0.04 times of the dry mass. The 1.0% dECM gel retracted approximately 85% after 21 days [$t(4) = 14$, $p < 0.001$], to 0.60 ± 0.27 times the dry mass, insignificantly different from the CHA control [$t(2) = 2.0$, $p = 0.19$]. After 21 days, the contraction of the 1.5% dECM hydrogel brought the swelling ratio to a comparable level to that of the control [$t(2) = .18$, $p = .87$], for an approximate 78% reduction in the swelling ratio [$t(4) = 9.3$, $p = .0007$], or 0.98 ± 0.62 times the dry mass.

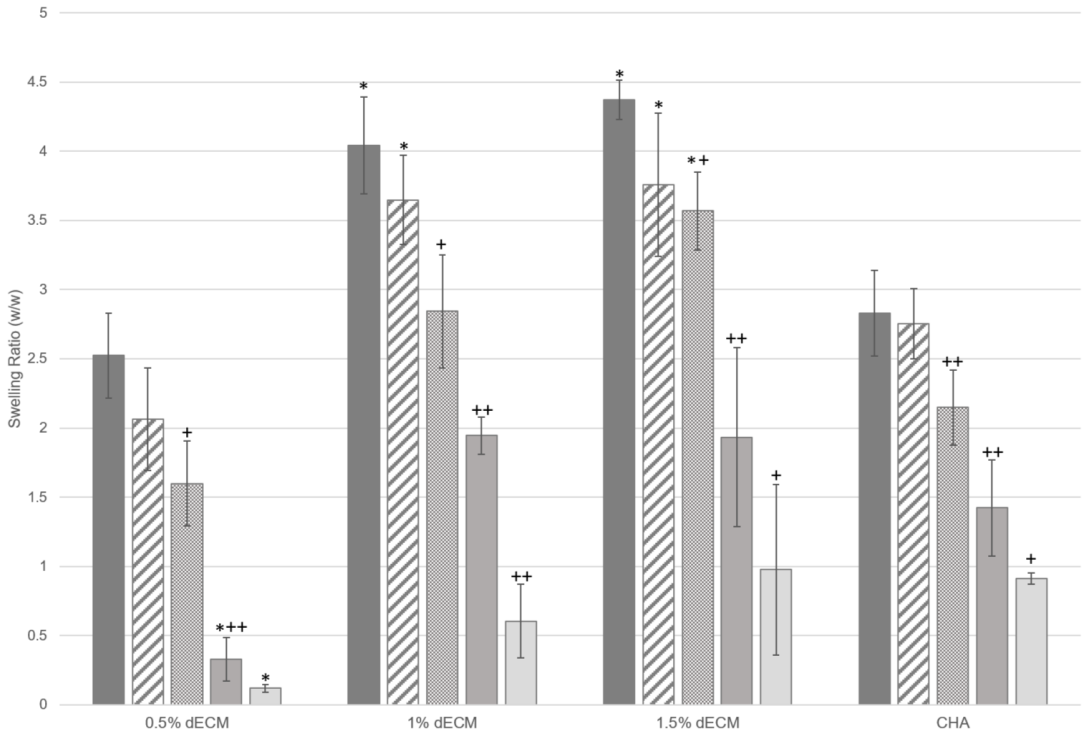

Figure 13. Hydrogel Swelling Kinetics. Swelling ratio (w/w) displayed as the mass fraction of the wet weight of each hydrogel after (■) 1 day; (▨) 4 days; (▩) 7 days; (■) 14 days; and (▭) 21 days of incubation at 37 ºC in PBS compared to its dry mass. Statistical significance determined by t-tests; n=3; (*) indicates a statistical difference in dECM hydrogel swelling ratio to the CHA control on the same day; (+) indicates contraction from the swelling ratio after day 1 by mass; (++) indicates further retraction compared to the previous time point.

Table 6. Average ± Standard Errors of Swelling Ratios (w/w)

	Day 1 (w/w)	**Day 4 (w/w)**	**Day 7 (w/w)**	**Day 14 (w/w)**	**Day 21 (w/w)**
0.5% dECM	2.5 ± 0.31	2.1 ± 0.37	1.6 ± 0.31	0.33 ± 0.16	0.12 ± 0.03
1.0% dECM	4.0 ± 0.35	3.6 ± 0.32	2.8 ± 0.41	2.0 ± 0.13	0.60 ± 0.27
1.5% dECM	4.4 ± 0.14	3.8 ± 0.52	3.6 ± 0.28	1.9 ± 0.65	0.98 ± 0.62
CHA control	2.8 ± 0.33	2.8 ± 0.25	2.2 ± 0.27	1.4 ± 0.35	0.91 ± 0.04

4.5. *In Vitro* Biocompatibility Assessment

4.5.1. Viability of Human VF Fibroblasts Encapsulated in dECM-hydrogels

Live/Dead staining was performed on HVFF after 1, 3, and 7 days of 3D encapsulation in 0.5%, 1.0%, and 1.5% dECM hydrogels, the CHA as negative controls, and 2D cultures on glass as positive controls respectively. Five images of each sample were taken with CLSM (**Figure 14A**), with images of the 3D hydrogels taken in 2D. Cell counting was performed manually using ImageJ. Three samples were used for each condition (**Figure 14B** and **Table 6**). In the glass positive control, live HVFF proliferated throughout the 7 days of the experiment, from 121 ± 33 per 1 mm^2 on day 1, to 161 ± 26 cells per mm^2 on day 3 [$t(13) = 3.2$, $p = .0074$], and 237 ± 22 on day 7 [$t(13) = 5.5$, $p = .0001$], a two-fold increase overall. HVFF cultured on glass exhibited typical, elongated fibroblast morphology throughout the culture period (**Figure 14A**). When encapsulated in CHA, HVFF also displayed similar fibroblast morphology. However, while cells initially appeared healthy, only an average 68 ± 20. live cells were counted per 1 mm^2 on day 3, compared to 100. ± 31 live cells on day 1 [$t(23) = 3.6$, $p = .0015$]. On day 7, the 72 ± 19 live cells counted were not significantly different from day 3 [$t(27) = .15$, $p = .88$].

In comparison to the CHA hydrogel, HVFF encapsulated in the dECM hydrogels demonstrated significantly less cell survival and proliferation and did not exhibit native fibroblast morphology (**Figure 14A**). After 1 day, only 14 ± 7.4 live HVFF per 1 mm^2 were counted for the 0.5% dECM hydrogel [$t(11) = 9.0$, $p < .0001$] and 9.7 ± 5.6 live HVFF in the 1.0% dECM hydrogel [$t(10) = 9.5$, $p < .0001$]. On day 3, proliferation was observed in both samples, up to four-fold increase in density (50 ± 16) for the 0.5% dECM [$t(27) = 6.9$, $p < .0001$] and five-fold (47 ± 14) for the 1.0% dECM [$t(18) = 9.6$, $p < .0001$], significantly greater than the number of live cells counted on day 1 in both cases. However, the number of dead cells also increased on day 3 in

both samples, to 51 ± 20. in the 0.5% dECM hydrogel and 34 ± 12 in the 1.0% dECM hydrogel, with cell nuclei stained red with propidium iodide. The increase in the number of dead cells was significant in both the 0.5% dECM hydrogel [$t(15) = 8.0$, $p < .0001$] and the 1.0% dECM hydrogel [$t(15) = 9.6$, $p < .0001$]. This indicated that the HVFF were dying, or not receiving enough nutrients to maintain a healthy equilibrium. On the 7th day, the number of live HVFF did not change significantly from day 3 for either the 0.5% dECM [$t(25) = 2.1$, $p = .051$] or the 1.0% dECM [$t(18) = 1.6$, $p = .12$] hydrogels. However, the number of dead cells in the 0.5% dECM hydrogel decreased to 25 ± 11 [$t(22) = 4.4$, $p = .00025$], and increased to 57 ± 35 [$t(17) = 2.3$, $p = .032$] in the 1.0% dECM hydrogel.

In the 1.5% dECM hydrogel, the greatest number of live cells was found after 1 day, 30. ± 6.1 per 1 mm^2. This value was significantly lower than the CHA hydrogel [$t(11) = 7.3$, $p < .0001$]. Notably, even on day 1, 23 ± 4.6 nuclei of HVFF encapsulated in the 1.5% dECM hydrogel were stained red, indicating the cells were dying. Although some cells died off to day 3, to a live cell count of 11 ± 3.4 HVFF per 1 mm^2 [$t(16) = 10.$, $p < .0001$], this trend did not continue to day 7. The live HVFF count on day 7 (24 ± 8.2) was not significantly different from day 1 [$t(25) = 2.0$, $p = .056$], but was significantly greater than day 3 ($t(19) = 6.0$, $p < .0001$). As a possible explanation for this inconsistency, it was noted during the experiment that the 1.5% dECM gels on day 3 had partially returned to a fibrillar state, which was not observed in the day 7 gels. This indicated a flaw in gel stability, possibly related to an error in the preparation process. The number of dead cells on day 7 (21 ± 6.1) was also not significantly different from day 1 [$t(28) = 4.3$, $p = .37$]. However, HVFF encapsulated in the 1.5% dECM hydrogel were noted as unhealthy throughout the experiment. One potential explanation was that dECM facilitated cell

survival, but low interconnectivity of the pores prevented sufficient nutrients and oxygen from reaching encapsulated cells within the gels and inhibited migration.

Based on this observation, the maximum thickness at which the cells used in this experiment would have received sufficient oxygen was calculated using a linear one-dimensional quasi-steady state approximation for the oxygen consumption rate of cells in a cylindrical hydrogel wherein oxygen transfer occurred between the hydrogel and media on solely the hydrogel's upper surface[85]. Maximum thickness was calculated from the derived **Eq. 3**:

$$T_{max} = \sqrt{\frac{2C_0 D}{\varphi}} \qquad \textbf{(Equation 3)}^{85}$$

Wherein T_{max} represented the maximum thickness, C_0 was the concentration of oxygen at the hydrogel-media interface, D was the diffusion constant of oxygen in DMEM (approximately 3 x 10^{-9} m^2/s), and φ was the metabolic consumption rate of oxygen by cells in culture. φ was assumed to be constant when cells were not dividing and was calculated using **Eq. 4**.

$$\varphi = m\rho \qquad \textbf{(Equation 4)}^{85}$$

In **Eq. 4**, m represented the metabolic rate of oxygen consumption per cell (6.07 x 10^{-17} mol/s/cell for human dermal fibroblasts, as the rate of oxygen consumption by HVFF specifically was not available)[86] and ρ was the average cellular density of the hydrogels (1.4 x 10^9 cells/L). C_0 was calculated from **Eq. 5**, wherein P represented the partial pressure of oxygen in DMEM (approximately 0.17 atm)[87], H was Henry's constant for DMEM (approximately 1000 L◦atm/mol)[88], and L was the depth of media covering the hydrogel, equivalent to the maximum thickness of the hydrogel.

$$C_0 = \frac{P}{H} - \frac{\varphi L^2}{D} \qquad \textbf{(Equation 5)}^{85}$$

Eq. 5 was substituted into **Eq. 3** with L = T_{max} to solve for the maximum thickness of the hydrogel, **Eq. 6**.

$$T_{max} = \sqrt{\frac{PD}{H\varphi}} \qquad \textbf{(Equation 6)}$$

When **Eq. 6** was solved, the maximum thickness at which HVFF throughout the hydrogel would have received sufficient oxygen was found to be 2.4 mm, 0.2 mm thinner than the hydrogels used in the experiment. Repeating the experiment with a smaller hydrogel volume would potentially ameliorate the oxygen deficiency, producing an environment more favorable to cell survival. As gels were imaged in 2D layers, it is possible the HVFF exited the CHA hydrogel and proliferated along its surface, potentially explaining the greater cell survival in comparison to the dECM hydrogels.

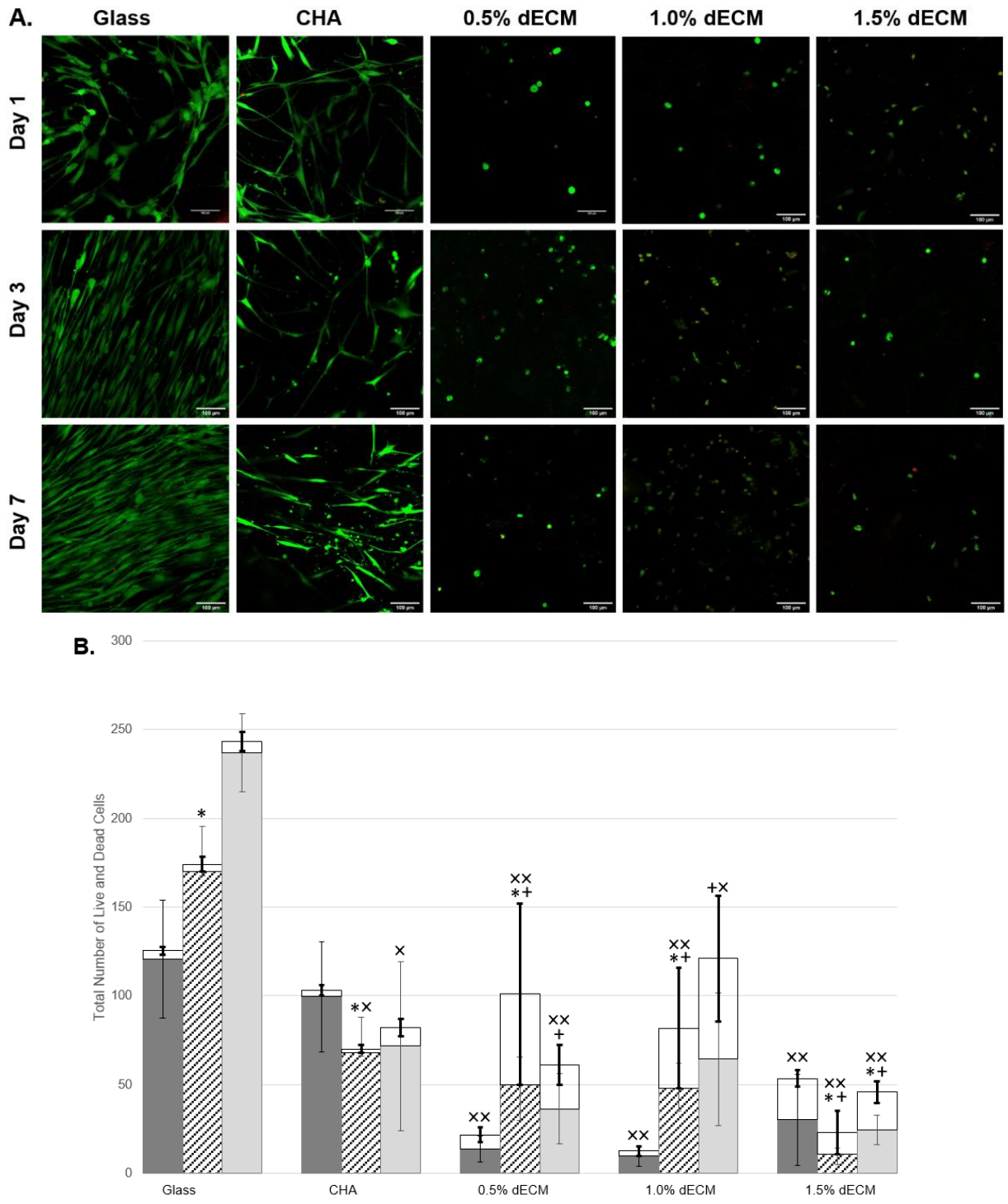

Figure 14. Human Vocal Fold Fibroblasts Viability. A. CLSM Imaging of Live Cells Stained with Calcein AM (green) and Dead Cells Stained with Propidium Iodide (red). B. Cellular Viability by Number of Live and Dead Cells Per 1 mm^2 Area. Cell 3D encapsulated

in dECM Hydrogels and the CHA hydrogel negative control, 2D culture on glass used as a positive control. Live cells on (■) Day 1; (▨) Day 3; (▩) Day 7. (□) Dead Cells; Assay conducted on n=3 gels per time point. Statistical significance determined by t-tests as $p < 0.05$. (*) indicates a statistical difference in number of live cells from previous time point for the same condition; (+) indicates statistical difference in number of dead cells from previous time point for the same condition; (x) indicates statistical difference in number of cells between a hydrogel and glass for the same time point; (xx) indicates a statistical difference in dECM gels with both CHA and glass for the same time point.

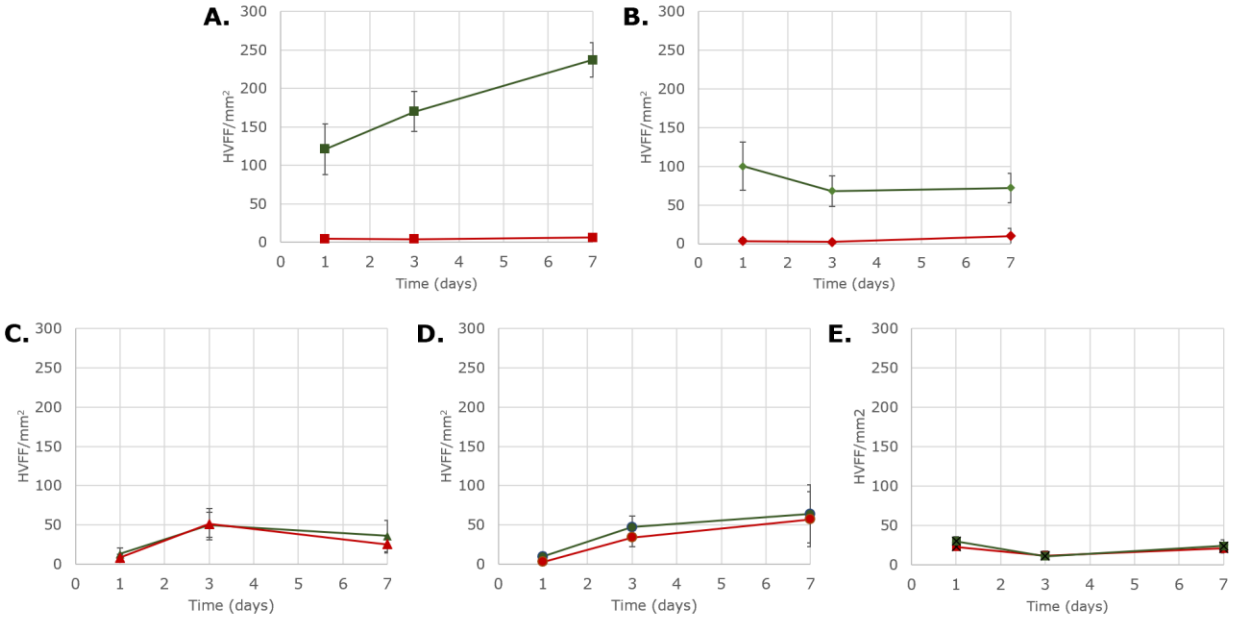

Figure 15. Number of Live and Dead Cells for Each Culturing Condition Over Time. (■) Live cells; (■) Dead Cells. (A.) Glass **(B.)** CHA Hydrogel **(C.)** 0.5% dECM Hydrogel **(D.)** 1.0% dECM Hydrogel **(E.)** 1.5% dECM Hydrogel.

4.5.2. Enzymatic Degradation Kinetics

After 3 h of incubation with 0.05% collagenase, less than 30% of the original mass remained for all three dECM concentrations. More specifically, the 0.5% dECM was reduced to 15.48 ± 5.42% residual mass, 1.0% to 21.94 ± 6.41%, and 1.5% to 28.62 ± 5.80% (**Figure 15**). No significant difference was found between the residual masses of the 0.5% and 1.0% dECM [$t(4) = 1.33$, $p = .25$], or the 1.0% and 1.5% dECM gels [$t(4) = 1.34$, $p = 0.25$]. However, the 0.5% dECM gel retained significantly lower residual mass compared to the 1.5% dECM gel [$t(4) = 2.87$, $p = .046$]. The CHA control also lost mass, to 41.97 ± 10.86% of the original mass. While the difference between the CHA and 1.5% [$t(4) = 1.88$, $p = .13$] and 1.0% [$t(4) = 2.75$, $p = .051$] dECM residual masses were insignificant, the CHA gel retained significantly greater mass than the 0.5% dECM gel [$t(4) = 3.78$, $p = .019$]. In contrast, the non-enzymatically degraded controls submerged in PBS lost some mass in lyophilization, to a residual mass of 92.57 ± 4.75%. This residual mass was significantly greater than that of the CHA control [$t(4) = 7.39$, $p = 0.0018$].

The decrease in residual mass slowed after the initial drop-off, with 4.41 ±3.72 % of the 0.5% dECM gel remaining after 12 h [$t(4) = 2.92$, $p = .04$], through degradation continued. At the same time point, 7.81 ± 2.30% of the 1.0% dECM gel [$t(4) = 3.59$, $p = .023$], 17.46 ± 3.43% of the 1.5% dECM gel [$t(4) = 2.87$, $p = .046$], and 18.03 ± 9.67% of the CHA gel [$t(4) = 2.85$, $p = .046$] remained, indicating that further degradation occurred after 3 h at a slower rate up to 12 h. Degradation of the 1.0% [$t(4) = 1.78$, $p = .15$] and 1.5% [$t(4) = .096$, $p = .93$] dECM hydrogels and CHA hydrogels continued at comparable rates. However, the residual mass of the 0.5% dECM hydrogel was no longer significantly different from the CHA [$t(4) = 2.28$, $p = .085$], yet was significantly lower than the 1.5% dECM gel [$t(4) = 4.47$, $p = .011$]. The non-enzymatically degraded dECM gel retained 86.72 ± 7.09 % of its initial mass, an insignificant decrease ($t(4) =$

1.19, p = .30) from the 3 h time point. The difference in residual mass between the CHA gel and non-enzymatically degraded dECM control remained significant [t(4) = 9.92, p = .00058].

After 60 h, the 0.5% dECM and CHA hydrogels were completely degraded, while 2.75 ± 0.80% of the 1.0% dECM gel and 10.97 ± 4.72% of the 1.5% dECM gel remained. The two residual gels were not statistically different in residual mass [t(2) = 2.97, p = .10]. The remainder of the 1.0% and 1.5% dECM hydrogels were completely degraded after 84 h. This additional time to degradation can likely be accounted for by the greater initial mass used in the fabrication of 1.0% and 1.5% dECM hydrogels at the same volume as the 0.5% dECM hydrogel. The non-enzymatically degraded gel still retained 81.80 ± 8.65% of its initial mass, and insignificant decrease likely caused by repeated lyophilization [t(4) = 1.89; p = 0.13]. As predicted, this residual mass is significantly higher than either the 1.5% [t(4) = 14.20, p = .00014] or 1.0% [t(2) = 18.51, p = .0029] dECM hydrogels. The presence of elastin and other ECM components that are less susceptible to collagenase degradation than collagen was likely the cause of the lengthened time to complete degradation for the 1.0% and 1.5% dECM hydrogels over the CHA hydrogel.

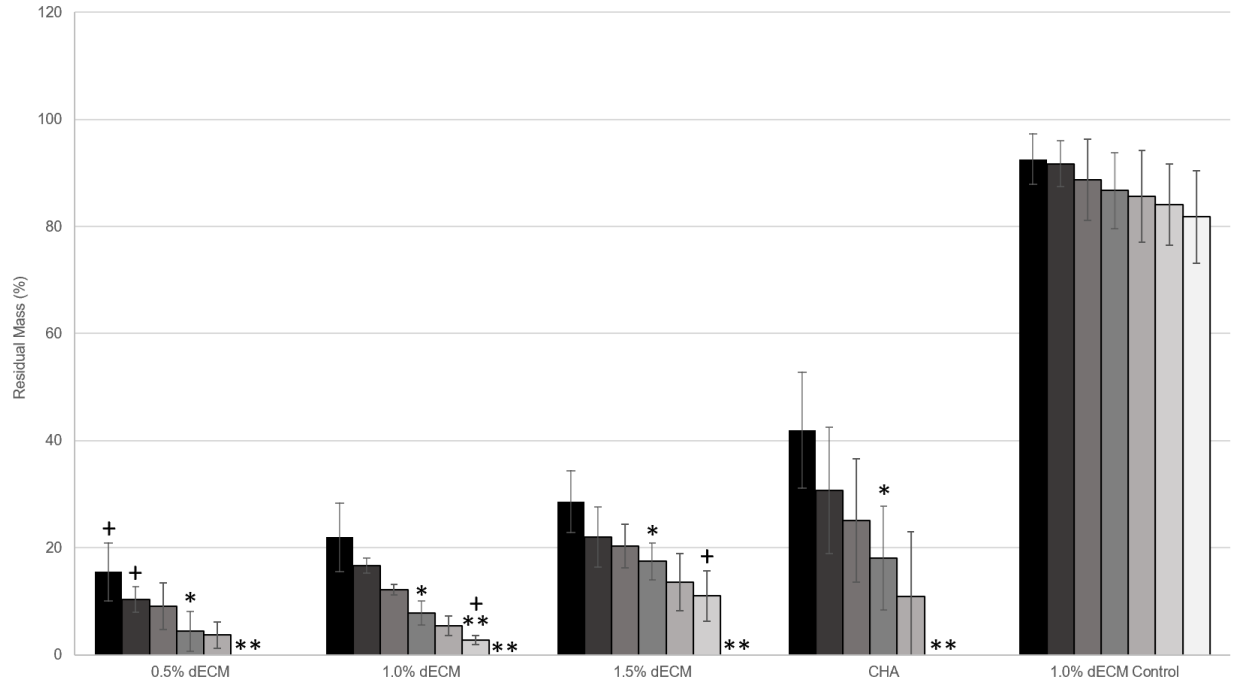

Figure 16. Degradation Kinetics as a Function of Residual Mass. Enzymatic degradation of 0.5% dECM, 1.0% dECM, 1.5% dECM, and CHA control hydrogels mediated by 0.05% collagenase over time periods of (■) 3 h; (■) 6 h; (■) 9 h; (■) 12 h; (■) 36 h; (■) 60 h, and (□) 84 h. A 1.0% dECM negative control incubated in PBS only was used to visualize the degree of degradation caused by lyophilization or natural protein degradation over the same period. Statistical significance was determined by t-tests for n = 3. (*) indicates a significant decrease from the residual mass after 3 h; (**) indicates a further significant decrease; (+) indicates a statistical difference between the residual mass of a dECM hydrogel and the CHA hydrogel.

Chapter 5. Summary of Scholarly Findings

Biomaterials such as dECM hydrogels that contain most components of native ECM have the potential to pave the way for the creation of bioactive, functional scaffolds for tissues with complex structure and unique biomechanical properties such as VF. Although scaffolds composed of whole VF dECM have previously been investigated for application in VF tissue engineering[3,12], these scaffolds must be surgically implanted, which can lead to inflammatory immune responses that can inhibit VF regeneration. Surgery can also lead to the formation of additional fibrotic tissue, worsening the voice disorder under treatment[16,23]. Theoretically, dECM hydrogels are injectable biomaterials that retain the bioactive properties and nanostructure of whole dECM scaffolds. In two previous studies, dECM hydrogels derived from SIS were evaluated for their potential to differentiate MSCs into HVFF and in a rat model[8,9]. However, in other tissues, including bone[7,10], cardiovascular tissue[5], muscle[54], and nerves[11], the source of dECM has been suggested to be essential for an effective remodeling response. By designing and evaluating a VF-derived dECM hydrogel in terms of biochemistry, mechanical properties, and biocompatibility, the applicability of such a material could be evaluated for VF tissue engineering.

A series of experiments were conducted on 0.5, 1.0, and 1.5% dECM hydrogels produced from homogenized dECM microparticles solubilized using pepsin. After a decellularization protocol was successful in removing greater than 95% of nucleic acids from VF, and a homogenization protocol selected to maximize dECM microparticle yield, the marker selected as a measure of effective decellularization[21], further biochemical analyses were necessary to determine the extent of compositional changes that occurred during decellularization and homogenization. Such compositional changes are unavoidable when using surfactants, but should be minimized[2]. While

no change was observed in total collagen concentration, normalized by percent of total protein, a slight decrease in elastin concentration occurred following homogenization. HA content was found to be reduced by both decellularization and homogenization, up to nearly 90%. This is greater than the up to 50% reduction in GAG content typically observed in tissues decellularized using surfactants[2].

Under ESEM, the dECM hydrogels were found to contain micropores no larger than 25 μm in diameter, with the majority under 5 μm. In contrast, the whole VF dECM was richly porous, with most pores ranging between 30-80 μm in diameter under ESEM. Results were in agreement with corresponding values in literature, in which pore sizes were reported between 10-100 μm in diameter for VF dECM[50]. The significantly smaller pores and lack of interconnectivity in the dECM hydrogels was a potential indicator of limited cellular survival upon 3D encapsulation as cellular migration might be inhibited. Additionally, increasing concentrations of dECM up to 1.5% appeared to create a more stable structure, with more defined pores and fully incorporated microparticles, in comparison to lower concentrations.

The elastic modulus of VF ranges between 0.1-1 kPa for humans and 1-3 kPa for pigs by linear shear rheometry[15]. It should be noted that linear shear rheometry is unable to provide a more definitive value for viscoelastic moduli of VF tissue due to tissue variability and VF behavior under strain is highly nonlinear. Of the three dECM concentrations, only the 1.5% dECM hydrogel achieved a storage modulus above the lower limit of the storage modulus of the human VF. Both the 1.5% and 1.0% dECM hydrogels gelled over a period of approximately 1 h, slower than the CHA control, which completed gelation in approximately 20 min. The storage modulus of the 1.0% and 1.5% dECM hydrogels also increased linearly with frequencies up to 10 Hz. However, the 1.0% dECM hydrogel did not achieve a deformation limit reliably greater than the

30% strain required for a biomaterial for VF tissue engineering[24], while the 0.5% and 1.5% dECM hydrogels did. In sum, only the 1.5% dECM hydrogel met the mechanical requirements for a VF biomaterial.

When HVFF were encapsulated in dECM hydrogels, the cells were not stimulated to elongate into typical fibroblast morphology, despite that such morphology was observed when HVFF were encapsulated in the CHA control. Additionally, HVFF encapsulated in the 1.5% dECM hydrogel were unhealthy or dying on day 1 after encapsulation, though a comparable number of unhealthy cells were counted at day 7. After 3 days, HVFF encapsulated in the 0.5% and 1.0% dECM hydrogels were observed to have entered the same unhealthy condition. Decreased concentrations of elastin and HA in the dECM microparticles are a possible contributing factor to the failure of HVFF to achieve a healthy, elongated morphology when encapsulated in dECM hydrogels. The small pore size and lack of pore interconnectivity observed in dECM hydrogels compared to whole dECM might also inhibit the ability of HVFF to receive sufficient oxygen and nutrients contained in media, hampering the cell viability. Alternatively, oxygen availability may have been limited due to the thickness of the hydrogel, and the difference may have been caused by HVFF exiting the CHA hydrogel and proliferating along the surface, while cell migration could not occur through the pores in the dECM hydrogels.

While 1.0% and 1.5% dECM hydrogels demonstrated greater initial swelling ratios compared to the CHA control, these gels did not overcome the flaw of collagen-based hydrogels and contracted to a smaller wet weight over a period of 21 days. When exposed to 0.05% collagenase, the 1.0% and 1.5% dECM hydrogels took 24 h longer to degrade than CHA and 0.5% hydrogels. However, this was likely due to the greater quantity of dECM in the higher concentration samples. For all dECM hydrogels and the CHA control, 100% degradation was

achieved in 3.5 days. The current VF-dECM only hydrogels do not overcome existing flaws of collagen and hyaluronic based hydrogels in VF tissue engineering, such as water loss over time and rapid degradation, without exhibiting a significant benefit in cellular biocompatibility. To meet the ultimate goal of VF regeneration, the VF-dECM only hydrogels will require significant modification of biochemical and mechanical properties in the design and fabrication process.

Chapter 6. Discussion, Study Limitations and Future Directions

As a summary, porcine VF were decellularized and homogenized into dECM microparticles less than 40 μm in diameter, and the extent of compositional changes to the ECM measured by quantification of collagen, elastin, and hyaluronic acid content. Significant reductions in elastin and hyaluronic acid content were found. Hydrogels were produced at dECM concentrations of 0.5, 1.0, and 1.5% by solubilization in a solution of pepsin and hydrochloric acid. To fabricate hydrogels, solubilized dECM was neutralized with sodium hydroxide, lyophilized, resuspended at the desired concentrations on ice, and incubated at 37 °C for 90 min.

Based on structural and mechanical characterization using ESEM and rheology, the 1.5% dECM hydrogel was most structurally sound and achieved viscoelastic properties most comparable to native human VF. However, the lack of large interconnected pores in the hydrogel likely impeded cellular survival and proliferation when HVFF were encapsulated and cultured over 7 days. Additionally, the contraction of dECM hydrogels incubated in PBS over time and rapid rate of degradation when exposed to collagenase did not present an improvement over the control CHA hydrogel or other existing biomaterials for VF tissue engineering. Although the dECM hydrogels developed herein are not readily applicable to VF tissue engineering as it is, modifications to improve pore size and long-term stability or reduce ECM alterations during homogenization have the potential to overcome these significant flaws of current materials.

The proposed bead milling homogenization protocol required repeated cycles of high frequency agitation to produce dECM microparticles, a process that generates heat. Although the process was conducted in a cold room, significant quantities of heat could still be generated, and no further heat controls were possible. This is a possible cause of alterations in dECM composition

due to homogenization, which could be limited by homogenization under more controlled conditions. Cryomilling is the most common homogenization method for dECM microparticle production prior to dECM hydrogel fabrication[7,10,63]. A cryomill was not available at McGill University for the research conducted in this thesis, leading to the use of the bead mill. The built-in temperature controls in a cryomill might help reduce the impact of heat generation on dECM microparticle composition, potentially leading to a higher yield without elastin reduction, or even help limit GAG reduction.

Using rheology, time to gelation is typically defined as the time at which the storage modulus becomes greater than the loss modulus. Because the storage modulus is always greater than the loss modulus for the dECM hydrogels, this method cannot give an accurate measure of gelation kinetics. An alternative measure can be given as the time at which the storage modulus stabilizes. However, this method did not give a gelation time for the 0.5% dECM hydrogel. Because the storage modulus was low and did not appear to increase when the 0.5% dECM pre-gel was incubated at 37 °C, the ability of this concentration dECM to form a gel was uncertain. A more accurate measure of gelation kinetics might be obtained from turbidimetric readings in a spectrophotometer, which can give both a highly specific time required for gelation and a formula for the rate of gelation[80].

The rapid degradation rate is another significant flaw in the VF dECM hydrogels, as the degradation rate remained comparable to an uncrosslinked CHA hydrogel. Ideally, the degradation rate of the hydrogel should match the rate of new ECM synthesis. Methods for decreasing the degradation rate of dECM hydrogels have been explored. For example, Wassenaar et al investigated methods to tune the degradation kinetics of dECM hydrogels, by crosslinking with glutaraldehyde or encapsulation and controlled release of doxycycline.

Although both changes lengthened degradation time *in vitro* and *in vivo*, only doxycycline did so without affecting biocompatibility and mechanical properties in a rat model[89].

A significant limitation of pepsin solubilized dECM hydrogels is the potential for complete or partial degradation of the bioactive molecules bound to dECM and denaturation of the tertiary structures of collagen and elastin. Urea extraction or crosslinking to form a composite are potential methods to eliminate the impact of pepsin solubilization on dECM and improve long-term stability. The production of dECM hydrogels by pepsin solubilization was compared with urea extraction from placenta ECM for bone tissue engineering [90]. Urea extraction involves processing dECM in a saline 2 M urea solution for 48 h at 4 ºC, followed by centrifugation to separate solubilized dECM from insoluble remnants. When urea extracted and pepsin solubilized dECM were used as hydrogel coatings on tissue culture plates to stimulate osteogenic differentiation of MSCs, the urea extracted hydrogel stimulated osteogenesis over the pepsin solubilized hydrogel.

One hypothesis was that urea-extracted dECM hydrogels would foster tissue-specific MSC differentiation over pepsin solubilized dECM hydrogels, and tested this hypothesis using photocrosslinkable dECM hydrogels containing 3D encapsulated MSCs[91]. In vitro studies showed that urea-extracted cartilage dECM hydrogels promoted MSC differentiation into chondrocytes, while pepsin solubilized dECM hydrogels did not[91]. As such, the photocrosslinking method used for hydrogel production could be potentially of interest for enhancing the efficacy of dECM hydrogels in VF tissue engineering.

Repeating the *in vitro* biocompatibility experiments with thinner hydrogels might produce more favorable results, based on the oxygen consumption rate calculations conducted after the experiments. However, due to the small pores in the dECM hydrogels, cell migration was likely

limited. Methods to improve porosity such as crosslinking the dECM to create an interconnected network of fibers should also be considered to improve the biocompatibility of the dECM hydrogels[50,92]. Crosslinking is frequently used to tune the mechanics of hydrogels. While common crosslinking agents present limits cell migration and may be cytotoxic, alternative, highly-specific crosslinking methods can be identified to tune the degradation and oscillatory properties of dECM hydrogels[33]. Crosslinking can be performed with dECM alone or in composite, without impairing the potential for tissue-specific cell-scaffold interactions. A non-cytotoxic crosslinking method may also help reduce the degradation rate of dECM hydrogels, to meet the rate of ECM deposition. The aforementioned photocrosslinking method was a potential method for enhancing the stability of dECM hydrogels, by adding UV crosslinking to the native thermoresponsive gelation of solubilized dECM[91]. Photocrosslinkable dECM hydrogels were formed by methacrylation of solubilized dECM, and stimulated chondrogenesis over dECM hydrogels produced by incubation at physiological temperature[93]. If a similar photocrosslinking method were applied to dECM hydrogels for VF tissue engineering, significant protocol optimization would be required to produce a hydrogel with the requisite mechanical properties, as VF are significantly less stiff than cartilage. Click-crosslinking may also present a method of crosslinking dECM hydrogels that has not previously been explored. Highly-specific click-crosslinking can proceed through Diels-Alder cycloaddition or thiol-ene addition without producing cytotoxic byproducts[33].

Composite hydrogels consisting of dECM and synthetic polymers have been predicted to improve the mechanical properties and degradation kinetics of dECM scaffolds while retaining their bioactive properties[3]. Anti-inflammatory Th-2 stimulation by bioactive molecules in dECM may also help ameliorate the potential for severe inflammatory response to synthetic polymers. A

three-component hydrogel consisting of a dECM base crosslinked with polyethylene glycol-linked HA was reported for neural tissue engineering[94]. These materials were selected to both replace HA lost in decellularization and improve the long-term stability of the dECM hydrogel. The combination hydrogel stimulated the extension of motoneurons over an HA gel alone, though a dECM-only gel was not tested.

Although VF possess unique anatomical and mechanical characteristics, established, clinically approved methods for creating materials from human VF, or biologically similar porcine VF, do not yet exist. This may account for the variability observed in biochemical analyses of ECM components, as well as the storage modulus, and swelling kinetics of the porcine VF dECM hydrogels described herein. This study represented the first attempt to develop a hydrogel derived from VF dECM. Future work can be to compare the VF-dECM hydrogels with those produced from SIS or UBM, commercially produced materials with established quality control protocols. Recommended next steps for production of a dECM hydrogel for VF tissue engineering are the development of a composite hydrogel produced by a non-toxic chemical crosslinking with the dECM component derived from SIS or UBM. Once this hydrogel was tuned to possess biomechanical properties comparable to native VF, a comparison could be made to a VF-derived dECM hydrogel produced using the same procedure, to determine the importance of ECM source in VF tissue engineering.

References

1 Chen, X. & Thibeault, S. L. Biocompatibility of a synthetic extracellular matrix on immortalized vocal fold fibroblasts in 3-D culture. *Acta biomaterialia* **6**, 2940-2948 (2010).

2 Keane, T. J., Swinehart, I. T. & Badylak, S. F. Methods of tissue decellularization used for preparation of biologic scaffolds and in vivo relevance. *J. Methods* **84**, 25-34 (2015).

3 Xu, C. C., Chan, R. W., Weinberger, D. G., Efune, G. & Pawlowski, K. S. A bovine acellular scaffold for vocal fold reconstruction in a rat model. *J Biomed Mater Res A* **92**, 18-32, doi:10.1002/jbm.a.32279 (2010).

4 Sadtler, K. *et al.* Proteomic composition and immunomodulatory properties of urinary bladder matrix scaffolds in homeostasis and injury. *Seminars in Immunology* **29**, 14-23, doi:https://doi.org/10.1016/j.smim.2017.05.002 (2017).

5 Claudio-Rizo, J. A. *et al.* Influence of residual composition on the structure and properties of extracellular matrix derived hydrogels. *J Materials Science Engineering: C* **79**, 793-801 (2017).

6 Badylak, S. F. *et al.* Esophageal preservation in five male patients after endoscopic inner-layer circumferential resection in the setting of superficial cancer: a regenerative medicine approach with a biologic scaffold. *Tissue Eng Part A* **17**, 1643-1650, doi:10.1089/ten.TEA.2010.0739 (2011).

7 Gibson, M. *et al.* Tissue extracellular matrix nanoparticle presentation in electrospun nanofibers. *Biomed Res Int* **2014**, 469120, doi:10.1155/2014/469120 (2014).

8 Huang, D., Wang, R. & Yang, S. Cogels of hyaluronic acid and acellular matrix for cultivation of adipose-derived stem cells: potential application for vocal fold tissue engineering. *BioMed research international* **2016** (2016).

9 Choi, J. W. *et al.* Small intestine submucosa and mesenchymal stem cells composite gel for scarless vocal fold regeneration. *Biomaterials* **35**, 4911-4918 (2014).

10 Beachley, V. *et al.* Extracellular matrix particle–glycosaminoglycan composite hydrogels for regenerative medicine applications. *Journal of Biomedical Materials Research Part A* **106**, 147-159 (2018).

11 Viswanath, A. *et al.* Extracellular matrix-derived hydrogels for dental stem cell delivery. *J Biomed Mater Res A* **105**, 319-328, doi:10.1002/jbm.a.35901 (2017).

12 Wrona, E. A. *et al.* Derivation and characterization of porcine vocal fold extracellular matrix scaffold. *The Laryngoscope* **126**, 928-935 (2016).

13 Hahn, M. S., Kobler, J. B., Starcher, B. C., Zeitels, S. M. & Langer, R. Quantitative and comparative studies of the vocal fold extracellular matrix I: elastic fibers and hyaluronic acid. *Annals of Otology, Rhinology & Laryngology* **115**, 156-164 (2006).

14 Hahn, M. S., Kobler, J. B., Zeitels, S. M. & Langer, R. Quantitative and comparative studies of the vocal fold extracellular matrix II: collagen. *Ann Otol Rhinol Laryngol* **115**, 225-232, doi:10.1177/000348940611500311 (2006).

15 Miri, A. K. Mechanical characterization of vocal fold tissue: a review study. *Journal of Voice* **28**, 657-667 (2014).

16 Li, L. *et al.* Tissue engineering-based therapeutic strategies for vocal fold repair and regeneration. *Biomaterials* **108**, 91-110 (2016).

17 Walimbe, T., Panitch, A. & Sivasankar, P. M. A review of hyaluronic acid and hyaluronic acid-based hydrogels for vocal fold tissue engineering. *Journal of Voice* **31**, 416-423 (2017).
18 Hahn, M. S., Kobler, J. B., Zeitels, S. M. & Langer, R. Quantitative and comparative studies of the vocal fold extracellular matrix II: collagen. *Annals of Otology, Rhinology & Laryngology* **115**, 225-232 (2006).
19 Madruga de Melo, E. C. *et al.* Distribution of collagen in the lamina propria of the human vocal fold. *The laryngoscope* **113**, 2187-2191 (2003).
20 Gaston, J. & Thibeault, S. L. Hyaluronic acid hydrogels for vocal fold wound healing. *Biomatter* **3**, e23799 (2013).
21 Wrona, E. A., Peng, R., Amin, M. R., Branski, R. C. & Freytes, D. O. Extracellular Matrix for Vocal Fold Lamina Propria Replacement: A Review. *Tissue Engineering Part B: Reviews* **22**, 421-429 (2016).
22 Ramig, L. O. & Verdolini, K. Treatment efficacy: voice disorders. *Journal of Speech, Language, and Hearing Research* **41**, S101-S116 (1998).
23 Mallur, P. S. & Rosen, C. A. Vocal fold injection: review of indications, techniques, and materials for augmentation. *Clinical and experimental otorhinolaryngology* **3**, 177 (2010).
24 Ling, C. *et al.* Bioengineered vocal fold mucosa for voice restoration. *Sci Transl Med* **7**, 314ra187, doi:10.1126/scitranslmed.aab4014 (2015).
25 Hu, X., Cebe, P., Weiss, A. S., Omenetto, F. & Kaplan, D. L. Protein-based composite materials. *Materials today* **15**, 208-215 (2012).
26 Hahn, M. S., Teply, B. A., Stevens, M. M., Zeitels, S. M. & Langer, R. Collagen composite hydrogels for vocal fold lamina propria restoration. *Biomaterials* **27**, 1104-1109, doi:https://doi.org/10.1016/j.biomaterials.2005.07.022 (2006).
27 Xu, W., Hu, R., Fan, E. & Han, D. Adipose-derived mesenchymal stem cells in collagen—hyaluronic acid gel composite scaffolds for vocal fold regeneration. *J Annals of Otology, Rhinology and Laryngology* **120**, 123-130 (2011).
28 Farran, A. J. *et al.* Effects of matrix composition, microstructure, and viscoelasticity on the behaviors of vocal fold fibroblasts cultured in three-dimensional hydrogel networks. *Tissue Engineering Part A* **16**, 1247-1261 (2010).
29 Hiwatashi, N. *et al.* The efficacy of a novel collagen–gelatin scaffold with basic fibroblast growth factor for the treatment of vocal fold scar. *J Journal of tissue engineering and regenerative medicine* **11**, 1598-1609 (2017).
30 Jetbumpenkul, P., Amornsudthiwat, P., Kanokpanont, S. & Damrongsakkul, S. Balanced electrostatic blending approach – An alternative to chemical crosslinking of Thai silk fibroin/gelatin scaffold. *International Journal of Biological Macromolecules* **50**, 7-13, doi:https://doi.org/10.1016/j.ijbiomac.2011.08.028 (2012).
31 Koob, T. J., Willis, T. A. & Hernandez, D. J. Biocompatibility of NDGA-polymerized collagen fibers. I. Evaluation of cytotoxicity with tendon fibroblasts in vitro. *J Biomed Mater Res* **56**, 31-39 (2001).
32 Moore, J. & Thibeault, S. Insights into the role of elastin in vocal fold health and disease. *Journal of Voice* **26**, 269-275 (2012).
33 Lau, H. K. & Kiick, K. L. Opportunities for multicomponent hybrid hydrogels in biomedical applications. *Biomacromolecules* **16**, 28-42 (2014).

34 Sionkowska, A., Skopinska-Wisniewska, J., Gawron, M., Kozlowska, J. & Planecka, A. Chemical and thermal cross-linking of collagen and elastin hydrolysates. *International journal of biological macromolecules* **47**, 570-577 (2010).
35 Haslik, W. *et al.* Management of full-thickness skin defects in the hand and wrist region: first long-term experiences with the dermal matrix Matriderm®. *Journal of plastic, Reconstructive & Aesthetic surgery* **63**, 360-364 (2010).
36 Min, J. H., Yun, I. S., Lew, D. H., Roh, T. S. & Lee, W. J. The use of matriderm and autologous skin graft in the treatment of full thickness skin defects. *Archives of plastic surgery* **41**, 330-336, doi:10.5999/aps.2014.41.4.330 (2014).
37 Saldin, L. T., Cramer, M. C., Velankar, S. S., White, L. J. & Badylak, S. F. Extracellular matrix hydrogels from decellularized tissues: Structure and function. *Acta Biomater* **49**, 1-15, doi:10.1016/j.actbio.2016.11.068 (2017).
38 Xu, C. C., Chan, R. W. & Tirunagari, N. A biodegradable, acellular xenogeneic scaffold for regeneration of the vocal fold lamina propria. *Tissue engineering* **13**, 551-566 (2007).
39 Kim, J. S., Kaminsky, A. J., Summitt, J. B. & Thayer, W. P. New Innovations for Deep Partial-Thickness Burn Treatment with ACell MatriStem Matrix. *Adv Wound Care (New Rochelle)* **5**, 546-552, doi:10.1089/wound.2015.0681 (2016).
40 Sicari, B. M. *et al.* An acellular biologic scaffold promotes skeletal muscle formation in mice and humans with volumetric muscle loss. *Sci Transl Med* **6**, 234ra258, doi:10.1126/scitranslmed.3008085 (2014).
41 Nevins, M. *et al.* The clinical efficacy of DynaMatrix extracellular membrane in augmenting keratinized tissue. *Int J Periodontics Restorative Dent* **30**, 151-161 (2010).
42 Mosala Nezhad, Z. *et al.* Small intestinal submucosa extracellular matrix (CorMatrix®) in cardiovascular surgery: a systematic review. *Interactive cardiovascular and thoracic surgery* **22**, 839-850, doi:10.1093/icvts/ivw020 (2016).
43 Slachman, F. N. Constructive Remodeling of CorMatrix Extracellular Matrix After Aortic Root Repair in a 90-Year-Old Woman. *The Annals of Thoracic Surgery* **97**, e129-e131, doi:https://doi.org/10.1016/j.athoracsur.2013.10.103 (2014).
44 Nieponice, A., Gilbert, T. W., Johnson, S. A., Turner, N. J. & Badylak, S. F. Bone marrow–derived cells participate in the long-term remodeling in a mouse model of esophageal reconstruction. *Journal of Surgical Research* **182**, e1-e7, doi:https://doi.org/10.1016/j.jss.2012.09.029 (2013).
45 Sutherland, A. J., Converse, G. L., Hopkins, R. A. & Detamore, M. S. The bioactivity of cartilage extracellular matrix in articular cartilage regeneration. *Adv Healthc Mater* **4**, 29-39, doi:10.1002/adhm.201400165 (2015).
46 Faulk, D., Johnson, S. & Badylak, S. in *Cardiac Regeneration and Repair* 180-200 (Elsevier, 2014).
47 Huber, J. E., Spievack, A., Ringel, R. L., Simmons-Byrd, A. & Badylak, S. Extracellular matrix as a scaffold for laryngeal reconstruction. *Ann Oto Rhinol Laryn* **112**, 428-433, doi:Doi 10.1177/000348940311200508 (2003).
48 Kitamura, M. *et al.* Glottic regeneration with a tissue‐engineering technique, using acellular extracellular matrix scaffold in a canine model. *J Journal of tissue engineering regenerative medicine* **10**, 825-832 (2016).
49 Pitman, M. J., Cabin, J. A. & Iacob, C. E. Small Intestinal Submucosa Implantation for the Possible Treatment of Vocal Fold Scar, Sulcus, and Superficial Lamina Propria

Atrophy. *Ann Otol Rhinol Laryngol* **125**, 137-144, doi:10.1177/0003489415601685 (2016).
50 Xu, C. C. & Chan, R. W. Pore architecture of a bovine acellular vocal fold scaffold. *Tissue Eng Part A* **14**, 1893-1903, doi:10.1089/ten.tea.2007.0243 (2008).
51 Xu, C. C., Chan, R. W., Weinberger, D. G., Efune, G. & Pawlowski, K. S. Controlled release of hepatocyte growth factor from a bovine acellular scaffold for vocal fold reconstruction. *J Biomed Mater Res A* **93**, 1335-1347, doi:10.1002/jbm.a.32632 (2010).
52 Tse, J. R. & Long, J. L. Microstructure characterization of a decellularized vocal fold scaffold for laryngeal tissue engineering. *Laryngoscope* **124**, E326-331, doi:10.1002/lary.24605 (2014).
53 Masaeli, E., Karamali, F., Loghmani, S., Eslaminejad, M. B. & Nasr-Esfahani, M. H. Bio-engineered electrospun nanofibrous membranes using cartilage extracellular matrix particles. *Journal of Materials Chemistry B* **5**, 765-776 (2017).
54 Ungerleider, J. L. *et al.* Extracellular Matrix Hydrogel Promotes Tissue Remodeling, Arteriogenesis, and Perfusion in a Rat Hindlimb Ischemia Model. *JACC Basic Transl Sci* **1**, 32-44, doi:10.1016/j.jacbts.2016.01.009 (2016).
55 Medberry, C. J. *et al.* Hydrogels derived from central nervous system extracellular matrix. *Biomaterials* **34**, 1033-1040, doi:10.1016/j.biomaterials.2012.10.062 (2013).
56 Su, M. C. *et al.* Measurement of adult vocal fold length. *J Laryngol Otol* **116**, 447-449, doi:10.1258/0022215021911257 (2002).
57 Bhattacharya, P. & Siegmund, T. A computational study of systemic hydration in vocal fold collision. *Comput Methods Biomech Biomed Engin* **17**, 1835-1852, doi:10.1080/10255842.2013.772591 (2014).
58 Zörner, S., Kaltenbacher, M. & Döllinger, M. Investigation of prescribed movement in fluid–structure interaction simulation for the human phonation process. *J Computers fluids* **86**, 133-140 (2013).
59 Prades, J. M. *et al.* Lamina propria of the human vocal fold: histomorphometric study of collagen fibers. *Surg Radiol Anat* **32**, 377-382, doi:10.1007/s00276-009-0577-9 (2010).
60 Kutty, J. K. & Webb, K. Tissue engineering therapies for the vocal fold lamina propria. *Tissue Eng Part B Rev* **15**, 249-262, doi:10.1089/ten.TEB.2008.0588 (2009).
61 Kurita, S. A comparative study of the layer structure of the vocal fold. *J Vocal fold physiology*, 3-21 (1981).
62 Smith, S. E. *et al.* Homogenized Porcine Extracellular Matrix Derived Injectable Tissue Construct with Gold Nanoparticles for Musculoskeletal Tissue Engineering Applications. *Journal of Biomaterials and Nanobiotechnology* **8**, 125 (2017).
63 Seo, Y., Jung, Y. & Kim, S. H. Decellularized heart ECM hydrogel using supercritical carbon dioxide for improved angiogenesis. *Acta biomaterialia* (2017).
64 Thibeault, S. L., Gray, S. D., Bless, D. M., Chan, R. W. & Ford, C. N. Histologic and Rheologic Characterization of Vocal Fold Scarring. *Journal of Voice* **16**, 96-104, doi:https://doi.org/10.1016/S0892-1997(02)00078-4 (2002).
65 Bitter, T. A modified uronic acid carbazole reaction. *Anal. Biochem.* **4**, 330-334 (1962).
66 Holmes, M., Bayliss, M. & Muir, H. Hyaluronic acid in human articular cartilage. Age-related changes in content and size. *Biochemical Journal* **250**, 435-441 (1988).
67 Cesaretti, M., Luppi, E., Maccari, F. & Volpi, N. A 96-well assay for uronic acid carbazole reaction. *Carbohydrate Polymers* **54**, 59-61 (2003).

68 Hahn, M. S., Kobler, J. B., Starcher, B. C., Zeitels, S. M. & Langer, R. Quantitative and comparative studies of the vocal fold extracellular matrix. I: Elastic fibers and hyaluronic acid. *Ann Otol Rhinol Laryngol* **115**, 156-164, doi:10.1177/000348940611500213 (2006).
69 Motta, A. *et al.* Fibroin hydrogels for biomedical applications: preparation, characterization and in vitro cell culture studies. *Journal of biomaterials science, Polymer edition* **15**, 851-864 (2004).
70 Annabi, N., Mithieux, S. M., Weiss, A. S. & Dehghani, F. The fabrication of elastin-based hydrogels using high pressure CO2. *Biomaterials* **30**, 1-7 (2009).
71 Schindelin, J. *et al.* Fiji: an open-source platform for biological-image analysis. *Nat Methods* **9**, 676-682, doi:10.1038/nmeth.2019 (2012).
72 Latifi, N., Asgari, M., Vali, H. & Mongeau, L. A tissue-mimetic nano-fibrillar hybrid injectable hydrogel for potential soft tissue engineering applications. *Scientific reports* **8**, 1047 (2018).
73 Zheng Shu, X., Liu, Y., Palumbo, F. S., Luo, Y. & Prestwich, G. D. In situ crosslinkable hyaluronan hydrogels for tissue engineering. *Biomaterials* **25**, 1339-1348, doi:https://doi.org/10.1016/j.biomaterials.2003.08.014 (2004).
74 Chen, X. & Thibeault, S. L. Novel isolation and biochemical characterization of immortalized fibroblasts for tissue engineering vocal fold lamina propria. *J. Tissue Engineering Part C: Methods* **15**, 201-212 (2008).
75 Wang, L. & Stegemann, J. P. Thermogelling chitosan and collagen composite hydrogels initiated with β-glycerophosphate for bone tissue engineering. *Biomaterials* **31**, 3976-3985, doi:https://doi.org/10.1016/j.biomaterials.2010.01.131 (2010).
76 Helling, A. *et al.* In vitro enzymatic degradation of tissue grafts and collagen biomaterials by matrix metalloproteinases: improving the collagenase assay. *J ACS Biomaterials Science Engineering* **3**, 1922-1932 (2016).
77 Kim, B. S., Choi, J. S., Kim, J. D., Choi, Y. C. & Cho, Y. W. Recellularization of decellularized human adipose-tissue-derived extracellular matrix sheets with other human cell types. *Cell Tissue Res* **348**, 559-567, doi:10.1007/s00441-012-1391-y (2012).
78 Stern, R. & Jedrzejas, M. J. Hyaluronidases: their genomics, structures, and mechanisms of action. *Chemical reviews* **106**, 818-839, doi:10.1021/cr050247k (2006).
79 Lee, W. & Toussaint, K. C., Jr. Quantitative analysis of the effect of environmental-scanning electron microscopy on collagenous tissues. *Sci Rep* **8**, 8491, doi:10.1038/s41598-018-26839-x (2018).
80 Wolf, M. T. *et al.* A hydrogel derived from decellularized dermal extracellular matrix. *Biomaterials* **33**, 7028-7038, doi:10.1016/j.biomaterials.2012.06.051 (2012).
81 Chan, R. W. & Rodriguez, M. L. A simple-shear rheometer for linear viscoelastic characterization of vocal fold tissues at phonatory frequencies. *J Acoust Soc Am* **124**, 1207-1219, doi:10.1121/1.2946715 (2008).
82 Ewoldt, R. H., Johnston, M. T. & Caretta, L. M. in *Complex fluids in biological systems* 207-241 (Springer, 2015).
83 Chan, R. W. & Titze, I. R. Viscoelastic shear properties of human vocal fold mucosa: measurement methodology and empirical results. *J Acoust Soc Am* **106**, 2008-2021 (1999).
84 Wei, Z. *et al.* Novel biocompatible polysaccharide-based self-healing hydrogel. *J Advanced Functional Materials* **25**, 1352-1359 (2015).

85 McMurtrey, R. J. Analytic Models of Oxygen and Nutrient Diffusion, Metabolism Dynamics, and Architecture Optimization in Three-Dimensional Tissue Constructs with Applications and Insights in Cerebral Organoids. *Tissue Eng Part C Methods* **22**, 221-249, doi:10.1089/ten.TEC.2015.0375 (2016).
86 Brown, M. F., Gratton, T. P. & Stuart, J. A. Metabolic rate does not scale with body mass in cultured mammalian cells. *American Journal of Physiology-Regulatory, Integrative, Comparative Physiology* (2007).
87 Zeitouni, N. E., Fandrey, J., Naim, H. Y. & von Kockritz-Blickwede, M. Measuring oxygen levels in Caco-2 cultures. *Hypoxia (Auckl)* **3**, 53-66, doi:10.2147/HP.S85625 (2015).
88 Vendruscolo, F., Rossi, M. J., Schmidell, W. & Ninow, J. L. Determination of oxygen solubility in liquid media. *ISRN Chemical Engineering* **2012** (2012).
89 Wassenaar, J. W., Braden, R. L., Osborn, K. G. & Christman, K. L. Modulating In Vivo Degradation Rate of Injectable Extracellular Matrix Hydrogels. *J Mater Chem B* **4**, 2794-2802, doi:10.1039/C5TB02564H (2016).
90 Kusuma, G. D. *et al.* Transferable Matrixes Produced from Decellularized Extracellular Matrix Promote Proliferation and Osteogenic Differentiation of Mesenchymal Stem Cells and Facilitate Scale-Up. *Acs Biomater Sci Eng* **4**, 1760-1769, doi:10.1021/acsbiomaterials.7b00747 (2018).
91 Rothrauff, B. B., Yang, G. & Tuan, R. S. Tissue-specific bioactivity of soluble tendon-derived and cartilage-derived extracellular matrices on adult mesenchymal stem cells. *Stem Cell Res Ther* **8**, 133, doi:10.1186/s13287-017-0580-8 (2017).
92 Vadodaria, K., Kulkarni, A., Santhini, E. & Vasudevan, P. Materials and structures used in meniscus repair and regeneration: a review. *Biomedicine-Taiwan* **9**, 11-22, doi:ARTN 2

10.1051/bmdcn/2019090102 (2019).
93 Rothrauff, B. B. *et al.* Efficacy of thermoresponsive, photocrosslinkable hydrogels derived from decellularized tendon and cartilage extracellular matrix for cartilage tissue engineering. *J Tissue Eng Regen Med* **12**, e159-e170, doi:10.1002/term.2465 (2018).
94 Thompson, R. E. *et al.* Effect of hyaluronic acid hydrogels containing astrocyte-derived extracellular matrix and/or V2a interneurons on histologic outcomes following spinal cord injury. *J Biomaterials* **162**, 208-223 (2018).